치의과학박사 학위논문

The role of PINK1 in osteoclast differentiation

PINK1 에 의한 파골세포 분화 조절에 대한 연구

2023 년 2 월

서울대학교 대학원

치의과학과 분자유전학 전공

홍 서 진

The role of PINK1 in osteoclast differentiation

PINK1에 의한 파골세포 분화 조절에 대한 연구

지도 교수 백 정 화 / 김 홍 희 / 이 장 희

이 논문을 치의과학박사 학위논문으로 제출함

2022 년 12 월

서울대학교 대학원

치의과학과 분자유전학 전공

홍 서 진

홍서진의 치의과학박사 학위논문을 인준함

2023 년 1 월

위 원 장 _____ (인)

부위원장 _____ (인)

위 원 _____ (인)

위 원 _____ (인)

위 원 _____ (인)

Abstract

The role of PINK1 in osteoclast differentiation

Seojin Hong
Program in Molecular Genetics
Department of Dental Science
The Graduate School
Seoul National University
Directed by Professor Jeong-Hwa Baek, D.D.S., Ph.D.,
Professor Hong-Hee Kim, Ph.D.,
Professor Zang-Hee Lee, D.D.S., Ph.D.

Periodontitis is a common chronic disease caused by bacteria in the oral cavity and accompanies an osteoclast-mediated gradual alveolar bone loss with dysfunctional mitochondria. Recent studies suggest that mitochondrial homeostasis is required for proper osteoclast differentiation. Defects in mitochondrial electron transport chain activity induce mitochondrial stress and activate the Ca^{2+}-calcineurin-mediated mitochondria-to-nucleus retrograde signaling, which eventually upregulates osteoclast differentiation.

Mitophagy is an essential cellular autophagic process that targets and degrades damaged mitochondria, protecting cells from oxidative stress. PINK1, a serine/threonine kinase, is involved in mitochondrial quality control via mitophagy. Although PINK1 has recently been implicated in preventing mitochondrial damage-induced excessive mitochondrial Ca^{2+} efflux and reactive oxygen species production, its precise role in osteoclast differentiation has not been elucidated.

In this study, I found that a lack of PINK1 accelerated alveolar bone loss in the ligature-induced periodontitis model. The μCT-analysis and TRAP staining of periodontal tissue demonstrated that an increase in the number of osteoclasts in *Pink1* knock-out mice contributed to the exacerbation of alveolar bone loss. The reduction in PINK1 expression led to mitochondrial dysfunction and mitophagy suppression, which turned on the osteoclastogenesis program by activating the NFATc1 pathway and increasing ROS production. I also found that the effects of deletion of *Pink1* on osteoclast formation could be relieved to some extent under an exogenous supply of the mitophagy stimulator, spermidine.

In summary, PINK1 positively affects proper osteoclast formation and maintenance of function through various regulations on mitochondria. This study may bring a novel therapeutic strategy, especially for periodontal disease with higher osteoclastic bone loss.

Keywords: Mitochondria, Mitophagy, NFATc1, Osteoclast, Periodontitis, PINK1

Student Number: 2016-22040

Table of Contents

List of Figures

List of Abbreviations

ATP	Adenosine triphosphate
Baf	Bafilomycin A1
BAX	Bcl-2-associated X protein
BMMs	Bone marrow macrophages
BSA	Bovine serum albumin
BV/TV	Bone volume/total volume
Ca^{2+}	Calcium
cGAS	Cyclic GMP-AMP synthase
CM-H_2DCFDA	2,7-dichlorofluorescein diacetate
DAPI	4′,6-diamidino-2-phenylindole
DAVID	Database for annotation, visualization and integrated discovery
DEG	Differentially expressed genes
ETC	Electron transport chain
FACS	Fluorescence activated single cell sorting
FBS	Fetal bovine serum
GO	Gene ontology
H&E	Hematoxylin and eosin
HBSS	Hanks' balanced salt solution
KO	Knock-out
LC3	Microtubule-associated protein 1 light chain-3B
LIP	Ligature-induced periodontitis
M1	Classically activated macrophage
M2	Alternatively activated macrophage
M-CSF	Macrophage colony stimulating factor
μ-CT	Micro-computed tomography
ΔΨm	Mitochondrial membrane potential
NAC	N-acetylcysteine
Oc.N/B.Pm	Osteoclast number/bone perimeter
Oc.S/B.S	Osteoclast surface/bone surface
OMM	Outer mitochondrial membrane
Parkin	Ubiquitin E3 ligase parkin

PBS	Phosphate-buffered saline
PI	Propidium iodide
PINK1	PTEN induced putative kinase 1
pOCs	Pre-fusion osteoclasts
RANKL	Receptor activator of nuclear factor-κB ligand
ROS	Reactive oxygen species
SD	Standard deviation
siRNA	Small interfering RNA
SPD	Spermidine
STING	Stimulator of interferon genes
Tb.Th	Trabecular thickness
TEM	Transmission electron microscopy
TRAP	Tartrate-resistant acid phosphatase
TRAP$^+$	TRAP-positive
Veh	Vehicle
WT	Wild type

The role of PINK1 in osteoclast differentiation

The contents will be published elsewhere as a partial fulfillment of Seojin Hong's Ph.D. program

I. Introduction

1.1. Bone remodeling and periodontitis

Bone is continuously remodeled throughout life, and this process is tightly regulated and maintained by homeostatic balance between the activity of bone-resorbing osteoclasts and the activity of bone-forming osteoblasts (Boyle et al. 2003; Florencio-Silva et al. 2015). Osteoclasts are multinucleated giant cells differentiated from monocyte-macrophage progenitors in response to the receptor activator of nuclear factor-κB ligand (RANKL), a member of the tumor necrosis factor family, and macrophage colony stimulating factor (M-CSF) (Soysa et al. 2012). Binding of M-CSF and RANKL to their respective receptors regulates osteoclast proliferation, differentiation, and survival. RANKL initiates calcium (Ca^{2+}) oscillations, which in turn activates the Ca^{2+}/calmodulin-dependent phosphatase, calcineurin (Kim and Kim 2014; Liu et al. 2020). Activated calcineurin induces dephosphorylation and nuclear translocation of nuclear factor of activated T cells (NFATc1), a master transcription factor of osteoclast differentiation. Activated NFATc1 upregulates the expression of representative osteoclast marker genes like *Acp5*, *Dcstamp*, *Ocstamp*, and *Atp6v0d2* (Figure 1) (Kim and Kim 2014; 2016).

Under normal conditions, bone homeostasis depends on the balance

between osteoclasts and osteoblasts activities. Due to excessive osteoclast resorption, inflammatory diseases such as periodontitis are often accompanied with osteolysis when this balance is disturbed (Chen et al. 2018; Kim et al. 2020). Periodontitis is a common chronic disease caused by bacteria in the oral cavity. The pathogenesis of periodontitis involves bacterial biofilm formation, which eventually challenges a host in the face of a significant inflammatory response in the oral environment (Sima et al. 2019). As the inflammation persists, osteoclast formation with high resorption activity is enhanced, resulting in severe destruction of alveolar bone and consequent loss of teeth (Graves et al. 2011). Although most periodontitis-related studies focus on bacterial-induced alveolar bone loss, it has recently been suggested that mitochondrial abnormalities and reactive oxygen species (ROS) production are also related to osteoclast dysfunction in periodontitis. (Angireddy et al. 2019; Bullon et al. 2012; Chen et al. 2019; Dobson et al. 2020; Liu et al. 2022). This suggests that exploring mechanisms linking mitochondrial dysfunction and osteoclasts may open new therapeutic avenues in the management of periodontitis.

1.2. Role of mitochondria in osteoclast regulation

Mitochondria is a double-membrane-bound organelle that is integral

in maintaining cellular homeostasis (Mohanraj et al. 2020). Since mitochondria sense and respond to rapid cellular adaptation to environmental shifts and produce energy, it is considered as important mediators of cell differentiation (Khacho et al. 2019; Seo et al. 2018; Shares et al. 2018). For example, the defects in mitochondrial electron transport chain (ETC) activity induce mitochondrial stress and activate Ca^{2+}-calcineurin-mediated mitochondria-to-nucleus retrograde signaling, which eventually upregulates osteoclast differentiation (Angireddy et al. 2019). A similar phenomenon was observed in the bone marrow macrophages (BMMs) from the *Mpv17* knock-out (KO) mouse model exhibiting mitochondrial DNA depletion (Angireddy et al. 2019), suggesting mitochondria is associated with osteoclast differentiation.

Mitochondria maintain their normal function by altering their mitochondrial dynamics such as (1) mitochondrial biogenesis, (2) fusion and fission, and (3) mitophagy (Ma et al. 2020). Recent evidence suggests that impaired mitochondrial quality regulation mediates changes in mitochondrial morphology, leading to defects in stem cell differentiation capacity (Cairns et al. 2020; Lin et al. 2021). In previous studies, we have reported that mitofusin 2 (mitochondrial fusion marker) act as a positive regulator in osteoclastogenesis through the Ca^{2+}-calcineurin-NFATc1 axis (Jung et al. 2019). The same phenomenon was observed in the dynamin-associated

protein 1 (mitochondrial fission marker) knock-downed macrophage, suggesting that both mitochondrial fusion and fission plays a pivotal role in regulating bone metabolism (Jeong et al. 2021). Whereas no differences in osteoclast differentiation was observed, a markedly reduced bone resorption was shown in mice with myeloid lineage-specific deletion of peroxisome proliferator-activated receptor gamma coactivators-1β (mitochondrial biogenesis marker that upregulates the local translation of mitochondrial proteins) (Zhang et al. 2018). Although the effects of mitochondrial biosynthesis, fusion, and fission are essential for osteoclast activation and formation, the role of mitophagy in osteoclast differentiation processes are still lacking.

1.3. PINK1, a regulator of mitochondrial function and quality

PTEN induced putative kinase 1 (*Pink1*) is a serine/threonine kinase identified as a causative gene in Parkinson's disease (Beilina et al. 2005; Quinn et al. 2020). PINK1 is involved in several cellular processes, particularly protecting cells from oxidative stress by degrading damaged mitochondria (Xiao et al. 2022). Several mechanisms for mitophagy regulation have been established, of which mitophagy mediated by PINK1 and the E3 ubiquitin-protein ligase parkin (Parkin) is perhaps the most well-

known pathway (Koyano et al. 2014; Lazarou et al. 2015). During PINK1-Parkin-mediated mitophagy, PINK1 is stabilized on the damaged mitochondrial outer membrane, triggers Parkin to translocate from the cytoplasm to the mitochondria, and activates its actions (Okatsu et al. 2015; Wauer et al. 2015). Activated Parkin induces mitochondrial outer membrane proteins ubiquitination (Gegg and Schapira 2011; Tanaka et al. 2010; Wang et al. 2011), followed by autophagy receptors recruitment, including optineurin (Lazarou et al. 2015), autophagosome formation via microtubule-associated protein 1 light chain-3B (LC3) interaction, and lysosome fusion. Through the forgoing process, PINK1-Parkin mediated mitophagy are formed, resulting in decomposition and removal of damaged mitochondria (Figure 2). Recently, the involvement of PINK1-dependent mitophagy in multiple myeloma has been studied. Multiple myeloma-induced *Pink1* KO mice showed poorer symptoms with higher bone loss than in the WT group, suggesting that PINK1-dependent mitophagy plays a critical role in the migration and homing of multiple myeloma cells in the bone marrow (Fan et al. 2020). Moreover, Lee et al. suggested that PINK1 activation controls mitochondrial quality with low ROS production playing a pivotal role in osteoblasts differentiation (Lee et al. 2021). These results suggest that PINK1 may also regulate the osteoclast through mitochondrial quality control such as mitophagy.

The mammalian mitochondrial ETC includes complexes I-IV and the electron transporters ubiquinone and cytochrome C (Zhao et al. 2019). In the respiratory chain of the mitochondrial inner membrane, the NADH-CoQ oxidoreductase (complex I) and ubiquinone-cytochrome C oxidoreductase (complex III) function to release electrons to produce ROS precursors (Bleier and Drose 2013; Zorov et al. 2014). Loss of ETC or altered membrane potential induces mitochondrial stress and increases cytosolic Ca^{2+} levels with activation of calcineurin, which enhances osteoclastogenesis (Angireddy et al. 2019; Guha et al. 2016). Apart from its role in mitophagy, PINK1 also regulates complex I activity by NDUFA10 phosphorylation (Morais et al. 2014; Pogson et al. 2014). In the absence of PINK1, functionally impaired mitochondria (Deas et al. 2009; Gautier et al. 2008; Sandebring et al. 2009) and increased calcium efflux from mitochondria through the mitochondrial Na^{+}/Ca^{2+} exchanger were observed, leading to higher Ca^{2+}-dependent phosphatase calcineurin activity (Gandhi et al. 2009). Collectively, by mediating the quality control of damaged mitochondria and directly regulating mitochondrial function, PINK1 may play an important role in maintaining mitochondrial homeostasis, which may subsequently influence osteoclast differentiation.

In this work, for the first time, I investigated the role of PINK1 in osteoclasts. Lack of PINK1 accelerated alveolar bone loss in ligature-induced

periodontitis (LIP) model. BMMs derived from *Pink1* KO mice were more prone to differentiation into osteoclasts with higher resorptive ability. The reduction in PINK1 expression leads to mitochondrial dysfunction, which turns on the osteoclastogenesis program by stimulating nuclear translocation of NFATc1, accompanied by increased cytosolic Ca^{2+} level. It was also found that pathophysiological effects under PINK1 deficient conditions could partially alleviated by spermidine (SPD), a natural mitophagy inducer. Here, I identify how PINK1 regulates osteoclast formation and proposes that restoration of impaired mitochondrial quality control in osteoclasts can be considered as a therapeutic strategy to maintain intact periodontal health.

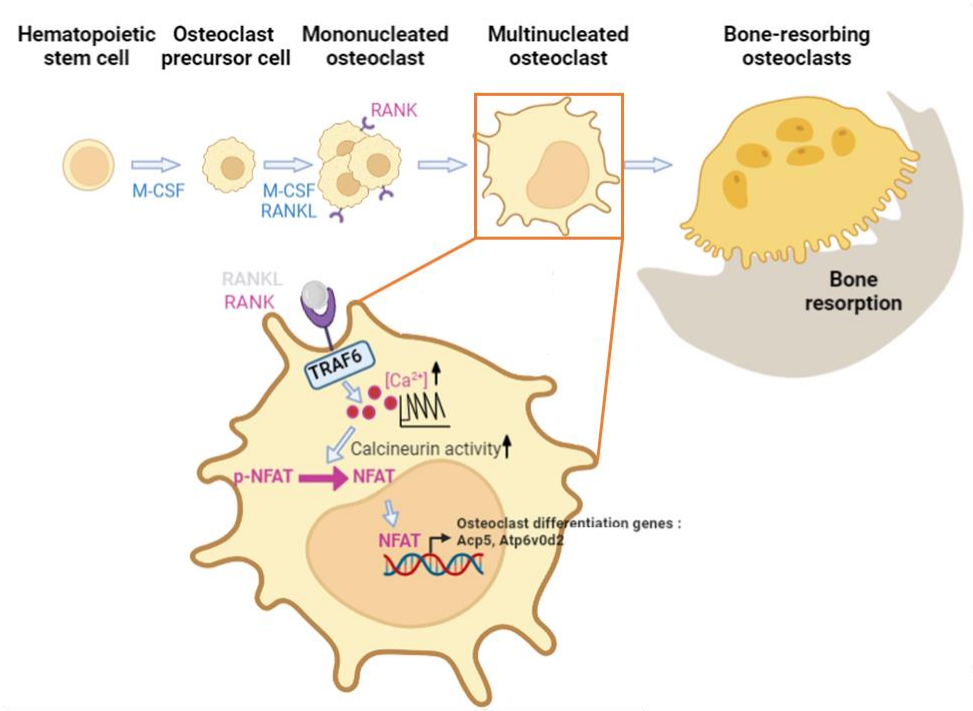

Figure 1. Schematic illustration of the Ca^{2+}-calcineurin-NFATc1 axis in osteoclastogenesis. Upon RANKL binding with RANK, TRAF6 is activated, leading to Ca^{2+} release from the endoplasmic reticulum and generating Ca^{2+} oscillation. Ca^{2+} oscillation induces the Ca^{2+}-calcineurin-NFATc1 axis. Dephosphorylated NFATc1 translocates into the nucleus and upregulate osteoclast-specific genes such as *Acp5* and *Atp6v0d2* (illustrated by using https://app.biorender.com).

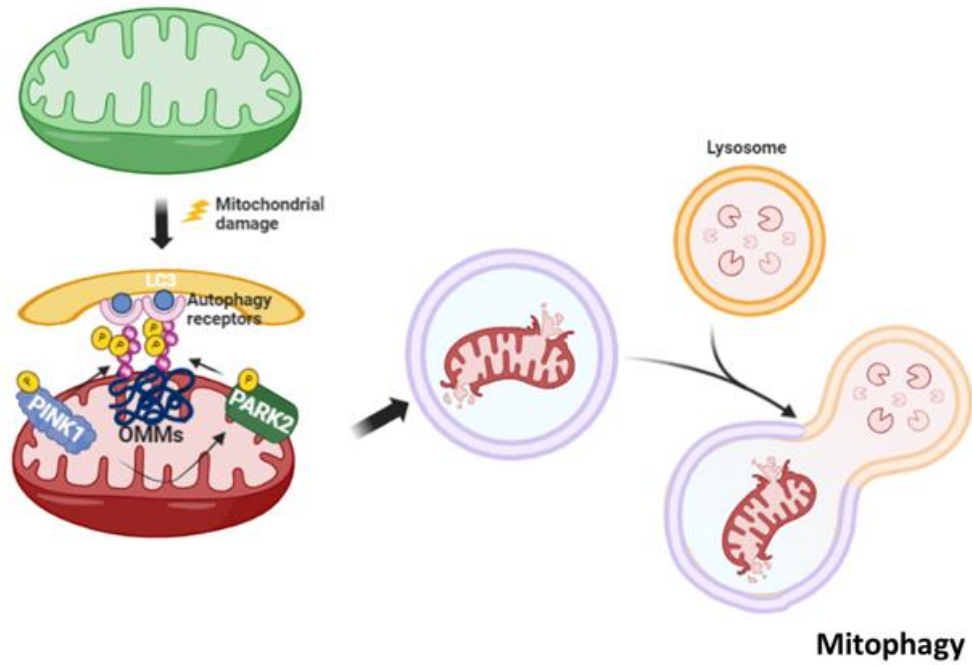

Figure 2. PINK1-dependent mitophagy. PINK1 accumulates on the outer mitochondrial membrane, forming homodimers and phosphorylating itself upon mitochondria depolarization. Recruited PINK1 phosphorylates Parkin and ubiquitin. E3 ubiquitin ligase activity of Parkin recruits more ubiquitin, auto-ubiquitinating itself and creating poly-ubiquitin chains on the damaged mitochondria surface. Consequently, these damaged mitochondria are being targeted to be degraded by mitophagy (illustrated by using https://app.biorender.com). OMMs, Outer Mitochondrial Membranes.

II. Materials and Methods

2.1. Animals

Pink1 KO were obtained from Chungnam National University College of Medicine (Shin et al. 2019). All mice were supplied with a regular diet and sterilized water and maintained in a specific pathogen-free animal facility at the Seoul National University School of Dentistry. All animal experiments were approved by the Institutional Animal Care and Use Committee at Seoul National University (SNU-211130-1-1 and SNU-201222-1-2) and performed under the approved guidelines.

2.2. Osteoclast differentiation

To generate osteoclasts, BMMs were prepared as previously described (Jung et al. 2019). Briefly, bone marrow cells were isolated from tibia and femurs of wild type (WT) or *Pink1* KO mice washed with α-MEM (Welgene, Daegu, Republic of Korea). Following lysis of red blood cells, the cells were cultured for 24 h in α-MEM containing 10% fetal bovine serum (FBS) and 30 ng/ml M-CSF. To obtain BMMs, non-adherent cells were collected and cultured on petri dishes with M-CSF for 3 days. BMMs were cultured for 2 or 4 days in

α-MEM containing 10% FBS with RANKL (100 ng/ml) and M-CSF (30 ng/ml) to generate pre-fusion osteoclasts (pOCs) or mature osteoclasts. Following differentiation of osteoclasts, cells were fixed in 4% paraformaldehyde for 15 min and permeabilized with 0.1% Triton X-100. Tartrate-resistant acid phosphatase (TRAP) staining was performed according to the manufacturer's instructions using a leukocyte acid phosphatase kit (Sigma-Aldrich, St. Louis, MO, USA). Cells were observed under a light microscope, and mature osteoclasts were defined as TRAP-positive ($TRAP^+$) cells with more than three nuclei.

2.3. Gene knock-down

BMMs were seeded at $3x10^4$ per well in 48-well plates or $3x10^5$ per well in 6-well plates. siRNA oligonucleotides (30 nM; Bioneer, Seoul, Republic of Korea) mixed with HiPerFect (Qiagen, Hilden, Germany) were transfected into BMMs for 6-14 h. The medium was then replaced with fresh complete α-MEM with M-CSF (PeproTech, Rocky Hill, NJ, USA) and RANKL (PeproTech) and cells were further cultured until the indicated days.

2.4. Real-time PCR

According to the manufacturer's instructions, total RNA was isolated from cells using TRIzol reagent (Invitrogen, Carlsbad, CA, USA). 3 μg RNA was used with Superscript II reverse transcriptase (Invitrogen) for cDNA synthesis. Amplified cDNA with SYBR Green Master Mix reagents (Applied Biosystems, Foster City, CA, USA) using an ABI 7500 instrument (Applied Biosystems). The mRNA expression level was evaluated according to the 2-ΔΔCT method and normalized to the *Hprt1* expression level. Primer sequences for real-time PCR were as follows: *Acp5*, 5'-CGA CCA TTG TTA GCC ACA TAC G-3' (sense), 5'-TCG TCC TGA AGA TAC TGC AGG TT-3' (antisense); *Atp6v0d2*, 5'-GGG AGA CCC TCT TCC CCA CC-3' (sense), 5'-CCA CCG ACA GCG TCA AAC AAA-3' (antisense); *Dcstamp*, 5'-GGG TGC TGT TTG CCG CTG-3' (sense), 5'-CGA CTC CTT GGG TTC CTT GCT-3' (antisense); *Fos*, 5'-ACT TCT TGT TTC CGG C-3' (sense), 5'-AGC TTC AGG GTA GGT G-3' (antisense); *Hprt1*, 5'-CCT AAG ATG AGC GCA AGT TGA A-3' (sense), 5'-CCA CAG GGA CTA GAA CAC CTG CTA A-3' (antisense); *Map1lc3b*, 5'-GAT AAT CAG ACG GCG CTT GC-3' (sense), 5'-ACT TCG GAG ATG GGA GTG GA-3' (antisense); *Mmp9*, 5'-GAC GGC ACG CCT TGG TGT AG-3' (sense), 5'-AGG AGC GGC CCT CAA AGA TG-3' (antisense); *Nfatc1*, 5'-CC AGTA TAC CAG CTC TGC CA-3' (sense), 5'-GTG GGA AGT CAG AAG TGG GT-3' (antisense); *Pink1*, 5'-TGA GGA

GCA GAC TCC CAG TT-3' (sense), 5'-CTT GAG ATC CCG ATG GGC AA-3' (antisense)

2.5. Western blotting

Cells were lysed in RIPA buffer (50 mM Tris-HCl, pH 8.0, 150 mM NaCl, 1% NP40, 0.1 % sodium dodecyl sulfate, 0.5% sodium deoxycholate, proteinase inhibitor cocktail, 0.5 mM PMSF, 1 mM NaF, and 1 mM Na_3VO_4) and centrifuged for 30 min at 14,000 rpm. Equal amounts of cell lysates were separated using 10 or 15% SDS-polyacrylamide gels and transferred to nitrocellulose membranes (GE Healthcare, Chalfont St. Giles, Buckinghamshire, UK). After blocking for 1 h with 5% fat-free milk/Tris-buffered saline, the membranes were incubated with a primary antibody and subsequently with a secondary antibody conjugated to horseradish peroxidase. Primary antibodies were used at 1:1,000 dilution to detect their corresponding proteins. Bound antibodies were identified using enhanced chemiluminescence reagents.

For mitochondrial fractions, the reagent-based protocol from the mitochondrial isolation kit (Thermo Fisher Scientific, Lafayette, CO, USA) was utilized.

2.6. *In vitro* bone resorption assay

BMMs obtained from WT or *Pink1* KO were cultured on dentin slices (Immunodiagnostic Systems, Boldon, UK) in α-MEM complete medium with M-CSF (30 ng/ml) and RANKL (100 ng/ml) for 12 days. Resorption pit depths of dentin slices were imaged and analyzed under Zeiss LSM 800 laser-scanning microscope (Carl Zeiss, Oberkochen, Germany). Representative images of the resorption area were obtained by the light microscopy and measured by ImageJ software (National Institutes of Health, Bethesda, MD, USA).

2.7. Bioinformatic analysis

BMMs from 2 biological replicates in each group (WT and KO) were cultured in α-MEM with M-CSF (30 ng/ml) and RANKL (100 ng/ml) until day 3. Total RNA was sent to ebiogen (Seoul, Republic of Korea) for quantum sequencing.

The GSE57468 data was obtained from Gene Expression Omnibus database (http://www.ncbi.nlm.nih.gov/geo/). logFC > 2 and P value < 0.05 were set as the thresholds for Differentially expressed genes (DEGs) screening. Statistically functional enrichment of clustered DEGs was analyzed by Database for Annotation, Visualization and Integrated Discovery (DAVID)

(https://david.ncifcrf.gov/, 6.7 version).

2.8. Transmission electron microscopy (TEM)

BMMs obtained from WT or *Pink1* KO were cultured for 2 days in α-MEM containing 10% FBS with M-CSF and RANKL to generate pOCs. pOCs were fixed with Karnovsky's fixative (2% glutaraldehyde, 2% paraformaldehyde, 0.5% $CaCl_2$) solutions, dehydrated and embedded in resin. Ultrathin sections were placed on a copper grid and double-stained with uranyl acetate and lead citrate to give contrast differences. Mitochondria image from pOCs were obtained using JEM-1011 TEM (JEOL, Tokyo, Japan) operating at 80 kV.

2.9. Measurement of ROS

BMMs were seeded at $6x10^4$ per well in 24-well plates or $3x10^5$ per well in 6-well plates. For the measurement of intracellular or mitochondrial ROS production, BMMs were incubated with the serum-free medium with 10 μM 2,7-dichlorofluorescein diacetate (CM-H_2DCFDA; Invitrogen) or 5 μM MitoSOX™ (Invitrogen) at 37°C for 10 min. The fluorescence images were analyzed by confocal microscope (LSM-700, Carl Zeiss).

2.10. Mitochondrial membrane potential (ΔΨm) detection

ΔΨm in the mitochondria of pOCs was detected by using JC-1 dye (Biotium, Fremont, CA, USA) according to the manufacturer's instructions. In brief, WT or KO BMMs were seeded at $2x10^4$ per well in 96-well plates and incubated with JC-1 working solution at 37°C for 15 min. The fluorescence was detected with a confocal microscope (LSM-700, Carl Zeiss) (excitation at 590 nm and emission at 610 nm for red fluorescence and excitation at 490 nm and emission at 520 nm for green fluorescence).

2.11. Cytoplasmic Ca^{2+} measurement

BMMs were plated in 96-well plates at $6x10^4$ cells/well and exposed to 100 ng/ml RANKL for 48 h. Cells were washed and incubated with 5 μM Fluo-4-dye-loading solution (Invitrogen) in Hanks' balanced salt solution (Thermo Fisher Scientific) according to the manufacturer's instructions at 37°C for 30 min. After incubation with dye, the cells were washed and resuspended into Hanks' balanced salt solution. Fluorescent Ca^{2+} indicators were measured with excitation wavelengths at 488nm, and emissions at 505-530 nm. Ionomycin (10 μM; Sigma-Aldrich) was used as a stimulus.

2.12. Nuclear translocation of NFATc1

To detect nuclear translocation of NFATc1, BMMs isolated from WT and KO were cultured on a cover glass with RANKL (100 ng/ml) and M-CSF (30 ng/ml) for 2 days. Cells were serum-starved for 4 h and then stimulated with RANKL (500 ng/ml) for 15 min. Afterwards, cells were fixed using 3.7% formaldehyde and permeabilized with 0.1% Triton X-100 for 30 min at room temperature. Blocking was performed using 1% bovine serum albumin (BSA) in phosphate-buffered saline (PBS), followed by incubation with NFATc1 antibody (1:200; Santa Cruz Biotechnology, Santa Cruz, CA, USA) at 4 °C overnight. Fluorochrome-conjugated secondary antibody (1:200; Thermo Fisher Scientific) was subsequently incubated for 1 h. For nuclear counterstaining, 4′,6-diamidino-2-phenylindole (DAPI; Sigma-Aldrich) was applied. Fluorescence imaging was observed under LSM700 (Carl Zeiss). Quantitative analysis of the NFATc1 colocalization with DAPI was performed using the Image J software.

2.13. Fluorescence activated single cell sorting (FACS) analysis

pOCs from WT and KO stained with Annexin V-FITC/Propidium iodide (PI) apoptosis kit BD Biosciences (San Jose, CA, USA) according to manufacturer's guidelines. Apoptotic cells were detected by FACS with

$1x10^4$-cell readouts by using and LSR-Fortessa X-20 (BD Biosciences), and were analyzed by Flowzo software (TreeStar, San Carlos, CA, USA).

2.14. Translocation of Bcl-2-associated X protein (BAX) to mitochondria

To detect the translocation of BAX from the cytosol to mitochondria, BMMs isolated from WT and KO were cultured on a cover glass with M-CSF and RANKL to generate pOCs. Cells were fixed by adding 3.7% paraformaldehyde for 30 min, followed by a permeabilization step with 0.1% Triton X-100 for 30 min. Cells were blocked in PBS containing 1% BSA, then incubated with BAX antibody (1:200; Cell Signaling Technology, Beverly, MA, USA) and TOMM20 antibody (1:200; Santa Cruz Biotechnology) at 4°C overnight. Cells were washed and incubated with fluorochrome-conjugated secondary antibody (1:200; Thermo Fisher Scientific) for 1 h in the dark. DAPI was applied for nuclear counterstaining. The images were acquired in a confocal microscope (Carl Zeiss) at respective excitation and emission. Colocalization values were obtained by quantifying the colocalization of TOMM20 and BAX with Image J software.

2.15. Mitophagy assessment

To detect mitophagy, BMMs isolated from WT and KO were cultured on a cover glass with RANKL (100 ng/ml) and M-CSF (30 ng/ml) for 2 days. pOCs grown on glass coverslips were incubated with 0.5 nM Mitotracker Red CMXRos probe (Invitrogen) for 45 min during cell culture according to the manufacturer's instructions. Cells were washed in PBS and fixed with 3.7% paraformaldehyde for 15 min at room temperature and then permeabilized with 0.1% Triton X-100. After blocking with 1% BSA for 2 h, cells were incubated with the primary antibody against LC3 (Cell Signaling Technology) at 4°C for overnight. pOCs-bound primary antibodies were visualized with FITC-conjugated anti-rabbit secondary antibodies (Thermo Fisher Scientific), and nuclei were labeled with DAPI. After mounting, the fluorescence images were analyzed using a confocal microscope (LSM-700, Carl Zeiss).

2.16. Autophagy flux analysis

BMMs from WT and KO were seeded in 24-well plates with a microscopy cover glass and transfected with mRFP-GFP-LC3 (#84572; Addgene, Watertown, MA, USA) using polyfect reagent (Promega, Madison, WI, USA) for 4.5 h. After fixing with 3.7% paraformaldehyde, images of cells were obtained using a confocal microscope (LSM-700, Carl Zeiss). GFP^{-}/RFP^{+}

(red) puncta or GFP^+/RFP^- (green) puncta were counted for quantification of autophagic flux.

2.17. Ligature-induced periodontitis (LIP) model

The ligature method was conducted on male 11-week-old WT and *Pink1* KO mice for five days to induce periodontitis. Between the maxillary left first and second molars, 5-0 silk ligature was inserted, and knots were tied on both ends. The contralateral side of each mouse was left without ligature.

2.18. Micro-computed tomography (μCT) analysis and bone histology

Maxillary alveolar bones from WT (n = 10) and *Pink1* KO (n = 7) mice were harvested and scanned with a Skyscan 1273 μCT scanner (70 kV, 114 μA, 9 pixel size; Skyscan, Kontich, Belgium). Alveolar bones were centered on the circular region-of-interest with diameter of 100-pixel size and bone parameters were analyzed for 50 frames from crown-side, 0.1 mm below of cemento-enamel junction where alveolar bone crest of WT controls were found on average, to root-side by using CtAN software (Skyscan) at threshold range between 90-255. For histological study, fixed alveolar bone were

decalcified with 12% (w/v) ethylenediaminetetraacetic acid solution for up to 4 weeks. Decalcified bones were embedded in paraffin wax. Samples were cut into 6 μm with a Leica microtome RM2145 (Leica, Wetzlar, Germany) and were subjected to TRAP staining. The images of alveolar bone osteoclasts in interradicular septum area of maxillary second molar were detected using bright field microscopy, and histomorphometric analysis was carried out using OsteoMeasure software (Osteometrics, Decatur, CA, USA).

2.19. Statistical analysis

All quantitative data are shown as means ± standard deviation (SD). Statistical significance was determined using student's *t*-test between two groups. A $P\ value < 0.05$ was taken as significant.

III. Results

3.1. PINK1 is upregulated during osteoclast differentiation

I first evaluated whether RANKL can regulate *Pink1* expression levels during osteoclast differentiation from BMMs by real-time PCR and western blotting. *Pink1* mRNA expression was significantly increased in BMMs treated with RANKL for the indicated times (Figure 3A). Additionally, PINK1 protein levels were significantly increased during osteoclastogenesis (Figure 3B). I found that PINK1 was strongly induced during RANKL-driven osteoclast differentiation. These findings suggest that PINK1 might have crucial roles during osteoclast differentiation.

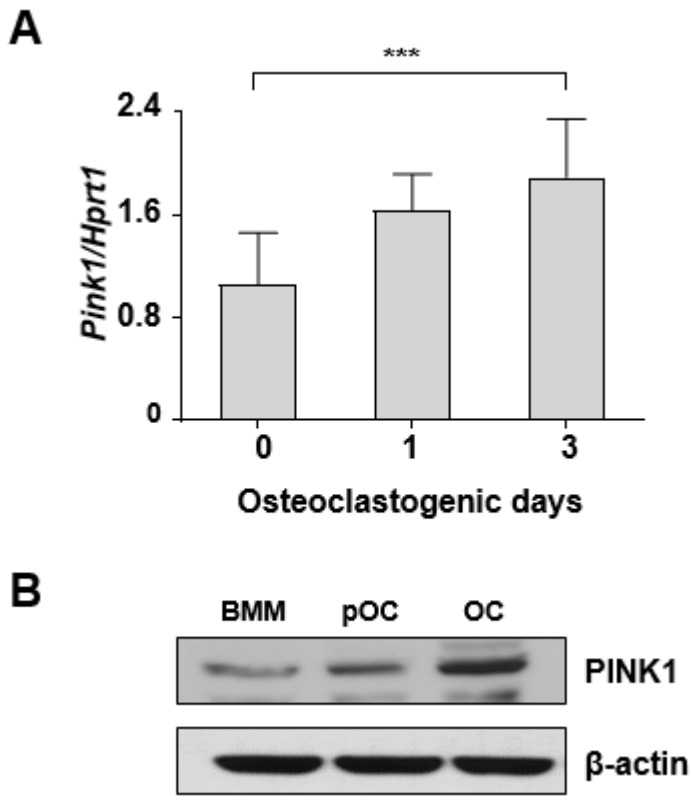

Figure 3. PINK1 is upregulated during osteoclast differentiation. (A) The mRNA levels of *Pink1* was analyzed by real-time PCR in BMMs cultured with RANKL and M-CSF for the indicated days. *** $P < 0.001$ versus D0. (B) BMMs were cultured in the osteoclastogenic conditions. Cell lysates were prepared and assessed by western blotting. The expression of β-actin was used as an endogenous control.

3.2. PINK1 negatively regulates osteoclast differentiation and function

To determine whether PINK1 is functionally involved in osteoclast differentiation, I knock-downed *Pink1* in BMMs by using siRNA and cultured the transfected cells with RANKL and M-CSF. A significant decrease in *Pink1* mRNA expression was observed (Figure 4A). In *Pink1* knock-down cells, the number of $TRAP^+$ multinucleated cells with more than 3 nuclei was increased and this increase was more pronounced in large $TRAP^+$ cells with more than 10 nuclei than in the control cells (Figure 4B). Consistent with these findings, RANKL treatment of PINK1 deficient BMMs caused a significant increase in the expression of representative osteoclast-associated marker genes, including *Fos, Nfatc1, Acp5*, and *Atp6v0d2* (Figure 5A). I next performed western blotting to analyze gene expression patterns at the protein level. *Pink1* knock-down induced upregulation of c-Fos and NFATc1 protein, master regulator genes of osteoclast differentiation, compared to the control group (Figure 5B). To clarify the role of PINK1 in osteoclast function, I determined the bone-resorption capacity of *Pink1* knock-downed BMMs on dentin discs. BMMs were cultured on dentin discs with RANKL and M-CSF until day 12 after transfection of either *Pink1* or control siRNAs. *Pink1* siRNA transfected osteoclasts showed significantly increased resorption area and pit depth, reflecting that PINK1 negatively acts in osteoclast activity (Figure 6).

I further explored the effect of PINK1 on osteoclast formation from BMMs of KO mice. At first, I verified that BMMs from *Pink1* KO mice had no *Pink1* expression at both the transcript and protein levels when cultured in the osteoclastogenic medium (Figure 7A). In line with *Pink1* knock-downed BMMs, *Pink1* KO group generated more multinucleated $TRAP^+$ cells than the WT group. Significantly fewer large $TRAP^+$ cells with more than 3 and 10 nuclei were seen in the WT group compared to the *Pink1* KO group (Figure 7B). Consistently, increased expression of osteoclast key marker mRNAs and proteins was observed in *Pink1* KO cells upon RANKL treatment (Figure 8). I next investigated whether enhanced osteoclast differentiation in *Pink1* KO cells accelerates bone resorption. Significant increases in resorption area and pit depth were observed in *Pink1* KO cells relative to WT, indicating higher resorbing activity of osteoclasts (Figure 9). Together, these data suggest that PINK1 is an essential negative regulator in osteoclast differentiation and its function.

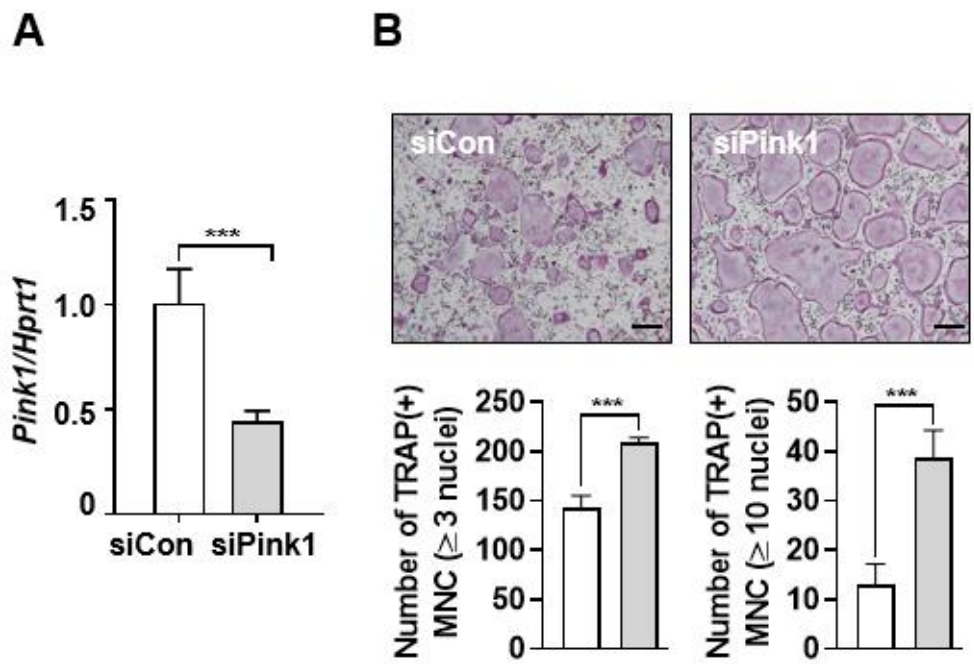

Figure 4. PINK1 deficiency regulates osteoclast differentiation of BMMs. (A) Knock-downed BMMs with either control or *Pink1* siRNA were further cultured in the presence of M-CSF (30 ng/ml) and RANKL (100 ng/ml). Total RNAs were prepared and analyzed by real-time PCR. (B) BMMs transfected with control or *Pink1* siRNA were further cultured with M-CSF and RANKL for 3 days. TRAP staining was performed and $TRAP^{+}$ multinucleated cells with more than 3 and 10 nuclei were counted. *** $P < 0.001$ versus control siRNA group. Scale bars, 200 μm.

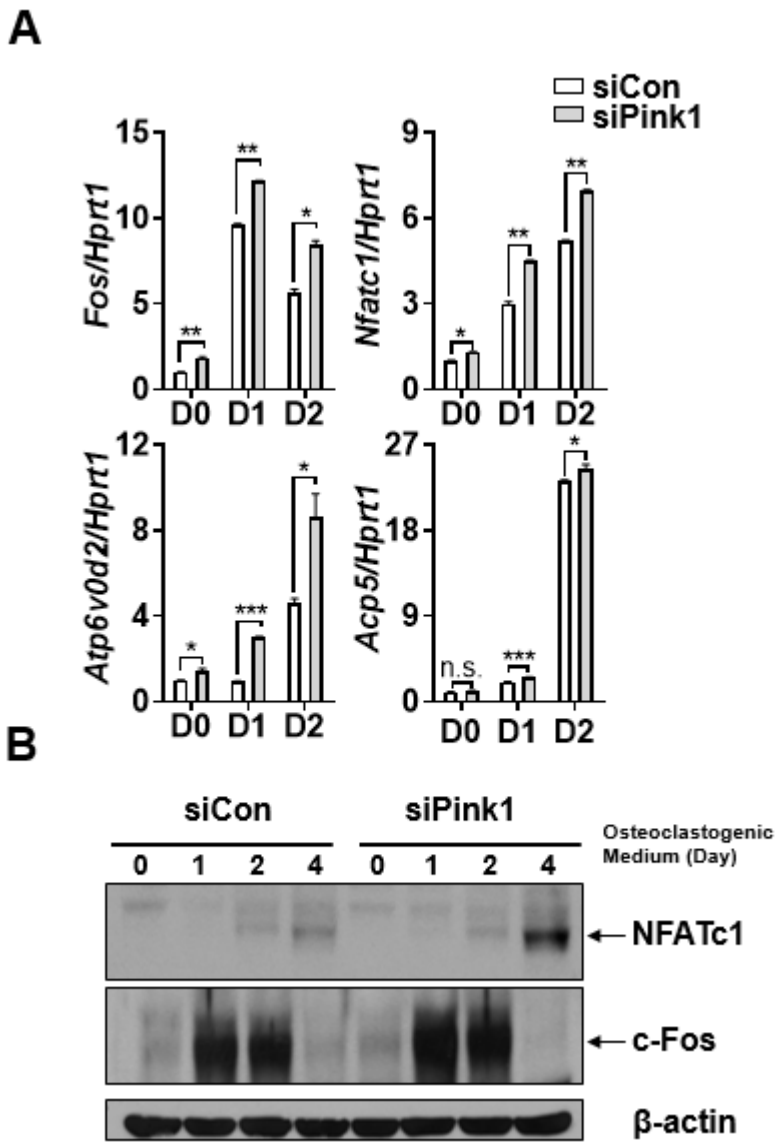

Figure 5. PINK1 deficiency enhances the expression of osteoclast-associated marker genes. (A) BMMs knock-downed with either control or *Pink1* siRNA were further cultured in the presence of M-CSF (30 ng/ml) and RANKL (100 ng/ml) for 1 or 2 days. The mRNA levels of osteoclast marker

genes were prepared from cells harvested and analyzed by real-time PCR. *Hprt1* expression level was used as an endogenous mRNA control in real-time PCR. * $P < 0.05$, ** $P < 0.01$, *** $P < 0.001$ versus control siRNA group. (B) BMMs transfected with control or *Pink1* siRNA were further cultured in the presence of M-CSF (30 ng/ml) and RANKL (100 ng/ml). Protein levels were examined by western blotting.

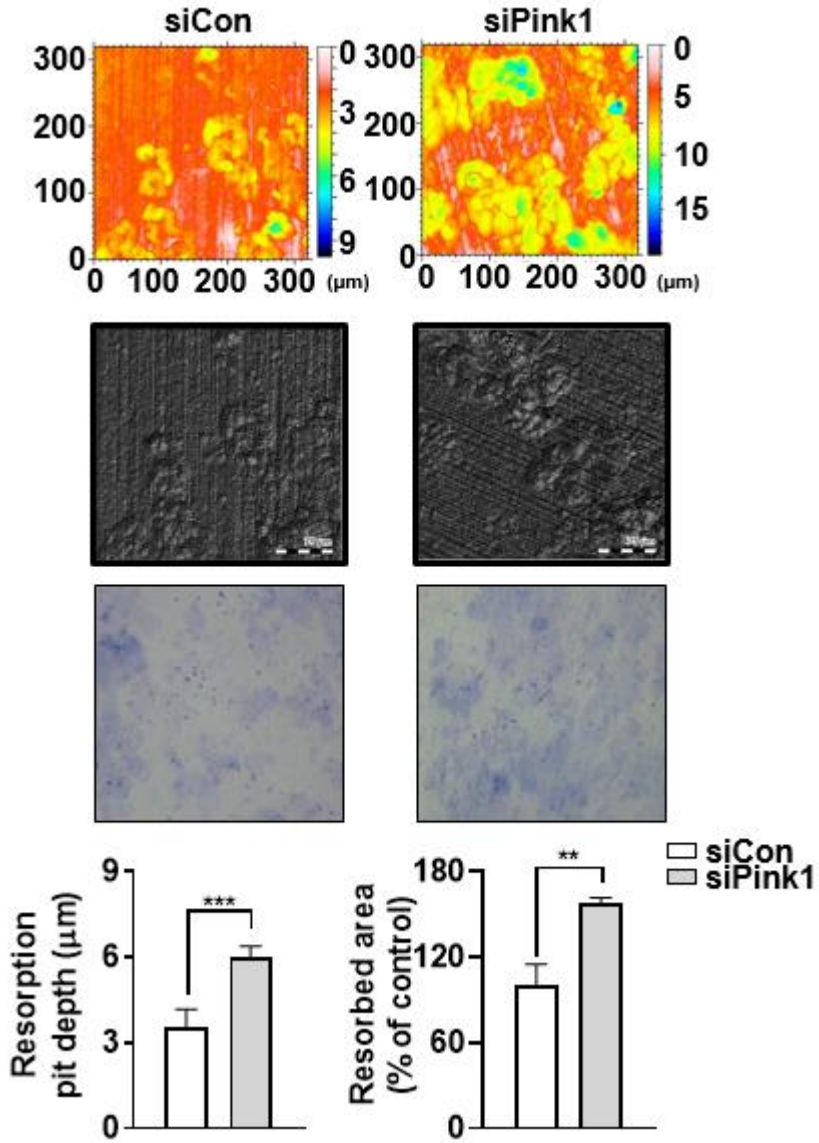

Figure 6. Downregulation of PINK1 enhances bone-resorption activity. BMMs transfected with *Pink1* or control siRNA on dentin disc were further cultured for 12 days with M-CSF and RANKL. Resorbed depth of dentin slices was assessed by confocal laser microscope. Scale bars, 75 μm. After

staining the dentin slices with trypan blue, the surface was photographed under the light microscopy and the total resorption areas were analyzed using the ImageJ software. The percentage of resorbed area and depth of resorption pits were presented as mean ± SD. ** $P < 0.01$, *** $P < 0.001$ versus control siRNA group.

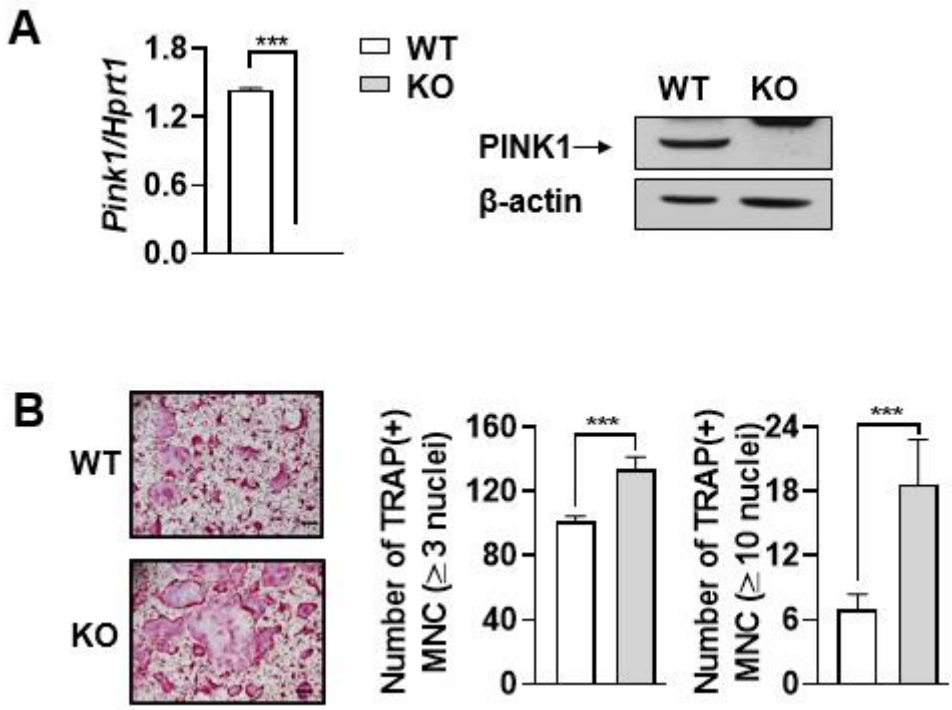

Figure 7. *Pink1* KO enhances osteoclast differentiation. (A) BMMs isolated from WT or *Pink1* KO mice were cultured with the osteoclastogenic medium. The RNA was analyzed by real-time PCR. The protein expression levels of PINK1 were analyzed by western blotting. β-actin was included as a loading control. (B) TRAP staining was performed and $TRAP^+$ multinucleated cells more than 3 and 10 nuclei were quantified. *** $P < 0.001$ versus WT group. Scale bars, 200 μm.

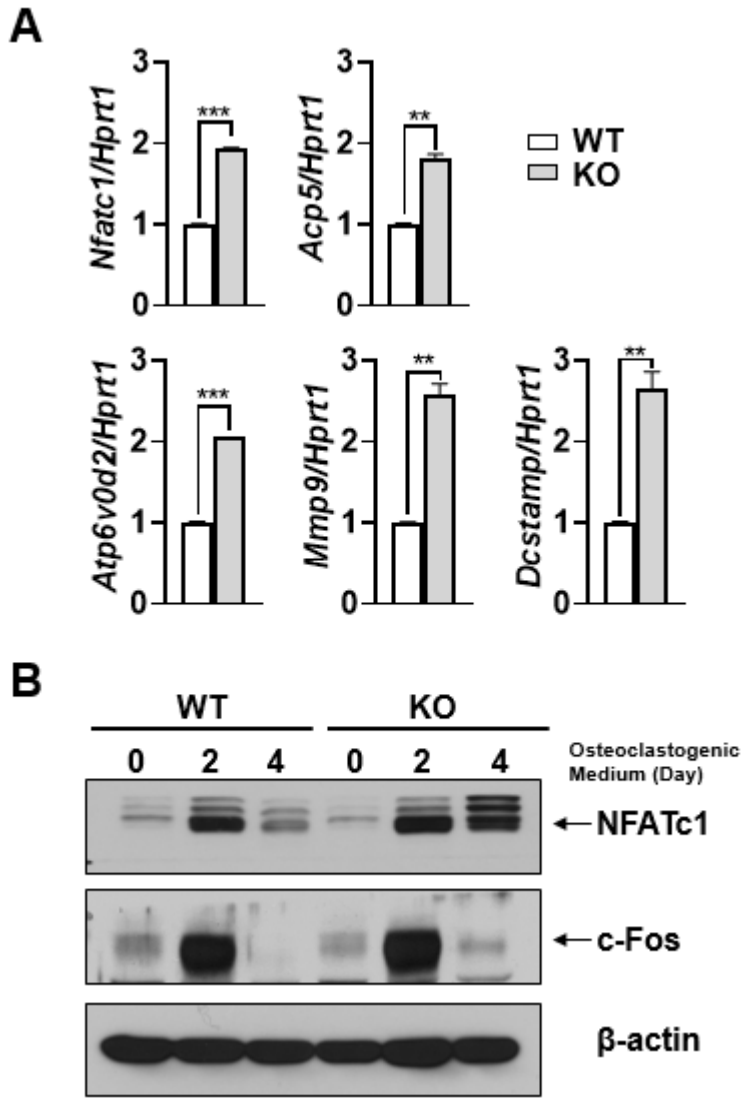

Figure 8. *Pink1* KO enhances the expression of osteoclast-associated marker genes. (A) BMMs harvested from either WT or *Pink1* KO mouse were further cultured in the presence of M-CSF (30 ng/ml) and RANKL (100 ng/ml) for 2 days. The mRNA levels of key osteoclast marker genes were determined by real-time PCR. ** $P < 0.01$, *** $P < 0.001$ versus WT group.

(B) WT or *Pink1* KO BMMs were cultured in the presence of M-CSF (30 ng/ml) and RANKL (100 ng/ml) for indicated days. The protein level of c-Fos and NFATc1 was assessed by western blotting. β-actin was included as a loading control.

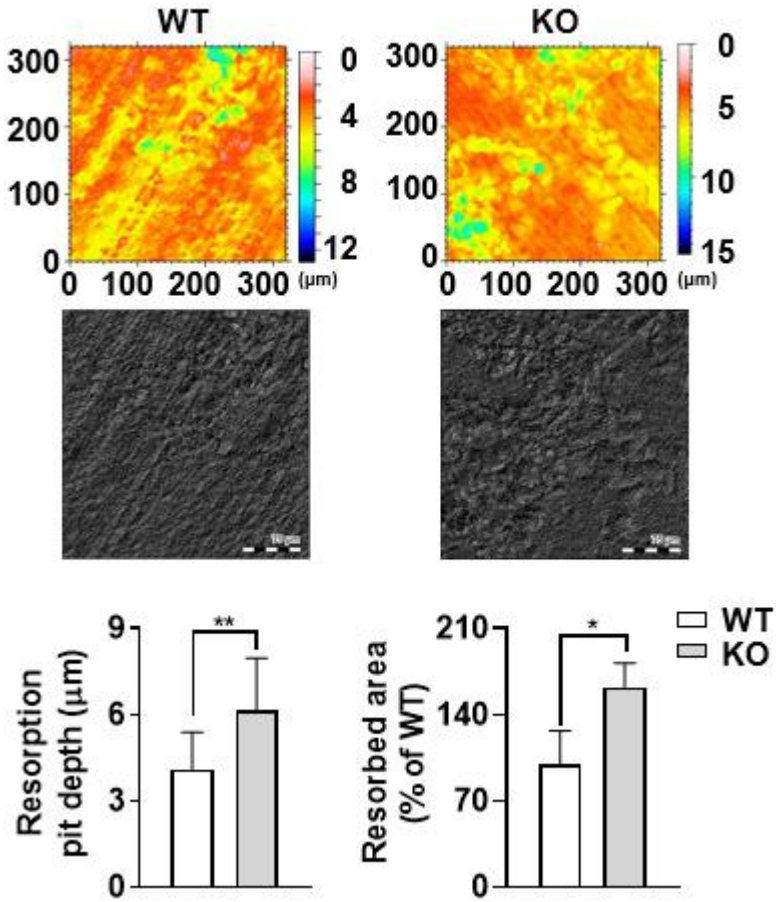

Figure 9. *Pink1* KO enhances bone-resorption activity. BMMs obtained from WT and KO mice were seeded on dentin slice and differentiated into osteoclasts with RANKL and M-CSF for 12 days. Representative dentine slices images were taken using confocal microscope. The percentage of resorbed area and depth of resorption pits were presented as mean ± SD. * $P < 0.05$, ** $P < 0.01$ versus WT. Scale bars, 75 μm.

3.3. PINK1 regulates osteoclastogenesis through the Ca^{2+}-NFATc1 axis.

It has been reported that calcium efflux from mitochondria increases under PINK1 deficient conditions (Lee et al. 2021). Since increased cytoplasmic Ca^{2+} levels activate NFATc1, a Ca^{2+}/calcineurin-dependent master regulator of osteoclastogenesis signaling (Negishi-Koga and Takayanagi 2009), I hypothesized that PINK1 negatively regulates osteoclastogenesis by controlling the Ca^{2+}-NFATc1 axis. I first examined the possibility of cytoplasmic Ca^{2+} as a mediator of PINK1 in regulation of osteoclast differentiation. *Pink1* WT and KO BMMs were cultured with RANKL and M-CSF for 2 days and incubated with Fluo-4/AM dye to determine cytoplasmic Ca^{2+} levels. As shown in Figure 10A, the cytoplasmic Ca^{2+} levels were significantly increased in *Pink1* KO cells than the WT cells. I next examined the effects of Ca^{2+} on the NFATc1 signaling pathway. In *Pink1* KO osteoclasts, decreased NFATc1 phosphorylation (Figure 10B) with elevated nuclear translocation of NFATc1 was observed (Figure 10C). Consistently, the increases in mRNA levels of *Nfatc1* downstream target genes were detected in PINK1-deficient pOCs (Figures 5A and 8A). Overall, the data show that PINK1 deficiency induced a higher propensity for osteoclast differentiation through activating the Ca^{2+}-NFATc1 signaling.

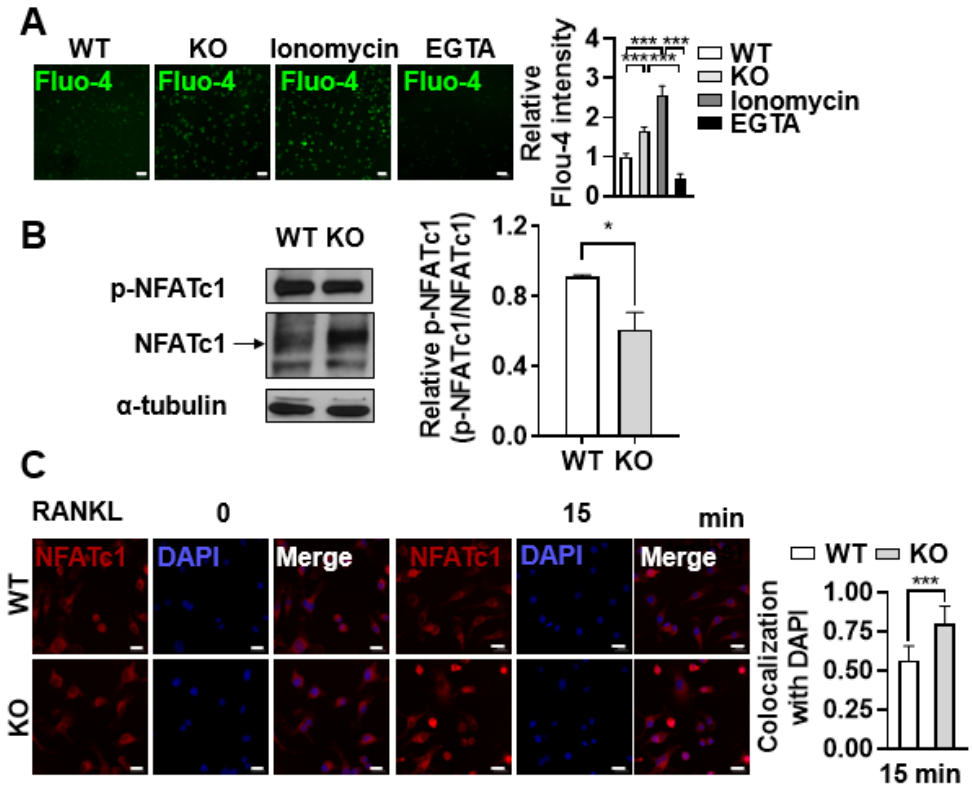

Figure 10. Upregulated cytosolic Ca^{2+} activates the NFATc1 signaling pathway. (A) BMMs isolated from WT and KO mice were plated on cover glasses and further processed for Fluo-4/AM staining. Stained cells were washed and measured with excitation wavelengths at 488 nm, and emissions at 505-530 nm under a confocal microscope. Scale bars, 50 μm. (B) BMMs from WT and KO mice were cultured in the osteoclastogenic conditions for 2 days and assessed by western blotting. Quantitative analysis of the phosphorylated NFATc1 to total NFATc1 level was performed using the Image J software. * $P < 0.05$ versus WT. (C) WT and KO pOCs were serum-

starved and stimulated with RANKL (500 ng/ml) for 15 min. Representative confocal images are presented. Scale bars, 20 μm.

3.4. PINK1 deficiency results in mitochondrial dysfunction during osteoclast differentiation

Since mitochondria sense and respond to environmental shifts for rapid cellular adaptation and produce energy, mitochondria are considered as important mediators of cell differentiation (Khacho et al. 2019; Seo et al. 2018; Shares et al. 2018). Recently, mitochondrial stress has been implicated in osteoclast differentiation (Angireddy et al. 2019; Guha et al. 2016; Srinivasan et al. 2010). In this study, PINK1 deficient group displayed higher osteoclast differentiation and resorption activity (Figures 4-9). Therefore, I considered the possibility that mitochondrial function and its dynamics are closely related to osteoclast differentiation. To gain some insight, I performed gene ontology (GO) enrichment analysis about mitochondrial dynamics by using publicly available datasets of BMMs undergoing osteoclastic differentiation (GSE57468) (An et al. 2014). The result indicated that several mitochondrial dynamics and roles including mitophagy changed during osteoclast differentiation (Figure 11A). Consistently, mitochondrial function-related mRNA levels were increased by M-CSF and RANKL treatment in my real-time PCR analyses (Figure 11B).

Given that the considerable mitochondrial dysfunction and impaired mitochondrial structure were shown in several PINK1-deficient cells (Deas

et al. 2009; Gautier et al. 2008; Sandebring et al. 2009), I decided to examine the morphology and dynamics of mitochondria in pOCs from WT and KO mice. TEM analyses showed severely damaged mitochondria in *Pink1* KO pOCs with loss of crista, enlarged vacuoles in matrix, and mitochondrial swellings (Figure 12). Given that decrease in ΔΨm favors Ca^{2+} efflux (Drago et al. 2011) and genetic deletion of *Pink1* led to an increase in intracellular Ca^{2+} content (Figure 10A), I assessed ΔΨm by JC-1 analysis as red-to-green ratio indicates the state of ΔΨm (Sivandzade et al. 2019). Mitochondria of *Pink1* KO pOCs displayed weak signals of red JC-1 aggregates, whereas similar signals of green JC-1 monomers were detected compared to control pOCs (Figure 13A). These results indicate that ΔΨm was disturbed under PINK1 deficient conditions. ROS, the by-product of oxidative phosphorylation, is often accompanied by loss of ΔΨm and release of Ca^{2+} in dysfunctional mitochondria (Ashrafi and Schwarz 2013). In line with mitochondrial abnormalities, both mitochondrial and intracellular ROS levels were significantly higher in KO pOCs than those in WT pOCs (Figure 13B). Overall, the data show that PINK1 deficiency altered mitochondrial integrity and function during osteoclast differentiation.

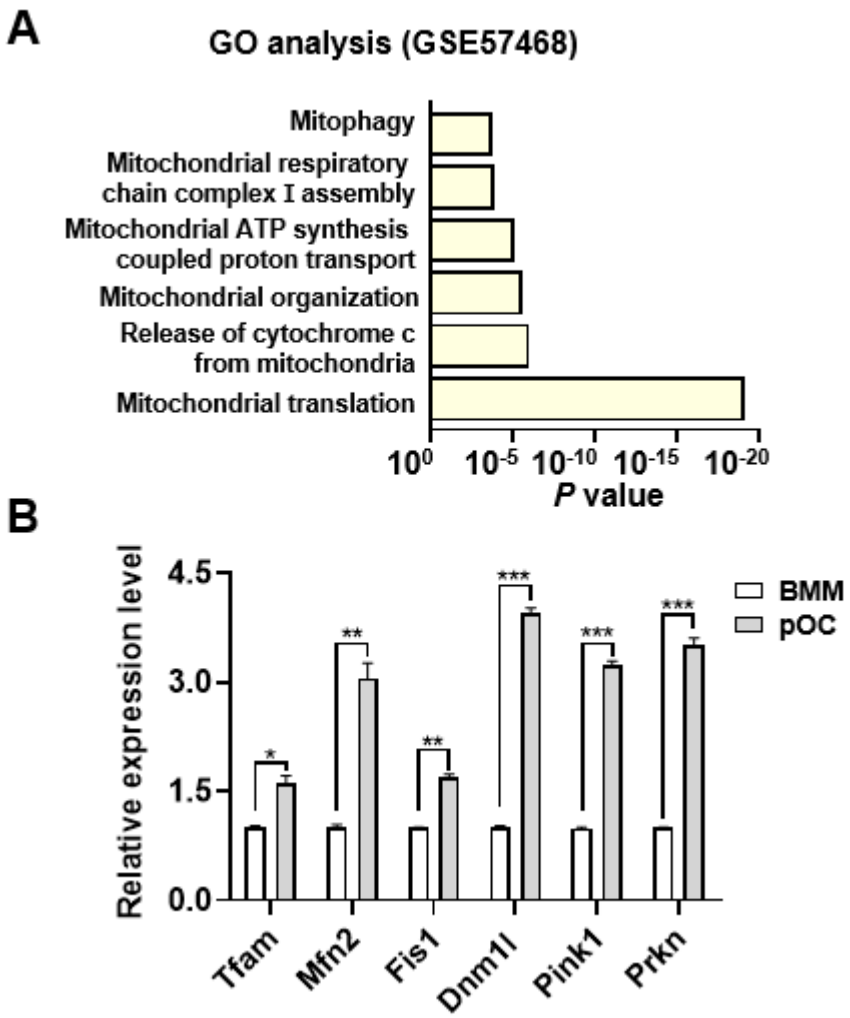

Figure 11. M**itochondrial dynamics changes during osteoclatogenesis.** (A) Enriched pathway analysis using the database of GSE57468. (B) The mRNA levels of key mitochondrial functional genes were determined by real-time PCR. * $P < 0.05$, ** $P < 0.01$, *** $P < 0.001$ versus BMMs.

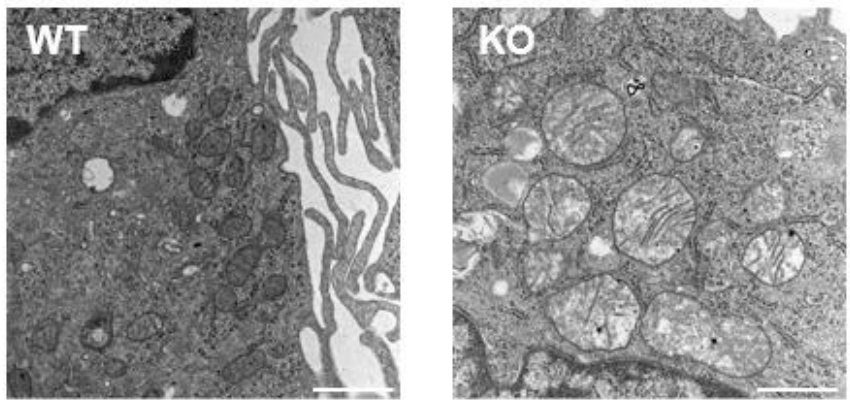

Figure 12. Representative TEM images of WT or KO pOCs. Cells were fixed, dehydrated, and then embedded in resin. Ultrathin sections were placed on a copper grid and negatively stained with uranyl acetate, followed by lead citrate staining. Representative mitochondria images of WT and KO pOCs were taken using JEM-1011 TEM. Scale bars, 1 μm.

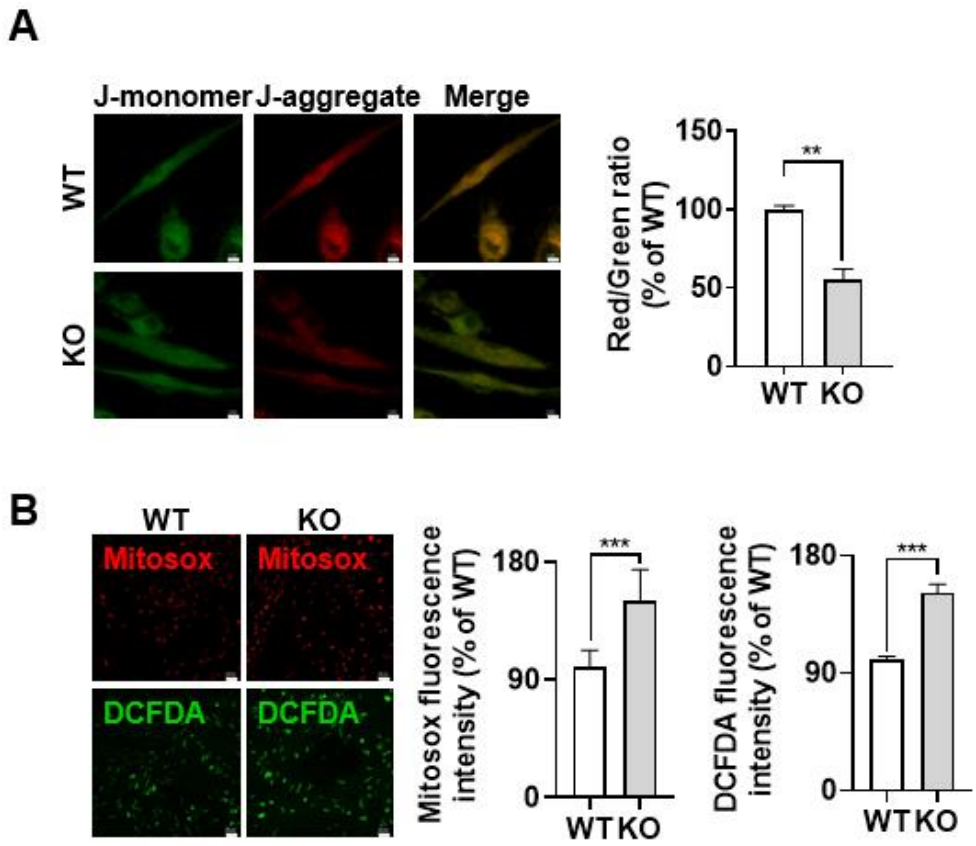

Figure 13. Relative ΔΨm and ROS in WT or KO pOCs. (A) BMMs isolated from WT or *Pink1* KO mice were cultured with the osteoclastogenic medium. pOCs were treated with JC-1 dye. After 15 min, cells were analyzed by the confocal microscopy. ** $P < 0.01$ versus WT. Scale bars, 5 μm. (B) WT or *Pink1* KO BMMs were cultured with the osteoclastogenic medium. pOCs were treated with CM-H_2DCFDA (10 μM) or MitoSOX™ (5 μM). After 15 min, cells were analyzed by a confocal laser scanning microscope to detect intracellular and mitochondrial ROS production. *** $P < 0.001$ versus WT. Scale bars, 50 μm.

3.5. Enhanced ROS accumulation partially augments osteoclast differentiation under PINK1-deficient conditions

ROS act as secondary messengers regulating osteoclast differentiation under physiological conditions (Ha et al. 2004). I therefore investigated whether hyperactivation of osteoclast differentiation in PINK1-deficient cells could be attenuated by scavenging excess ROS with N-acetylcysteine (NAC) treatment. Increased ROS accumulation was dramatically blocked by NAC addition (Figure 14A). Also, NAC treatment significantly reduced the number of multinucleated $TRAP^+$ cells and key osteoclastogenic marker expression in both WT and *Pink1* KO cells (Figure 14B-C). These results demonstrated that the enhancement of osteoclast differentiation in PINK1 deficiency is in part due to elevated ROS accumulation.

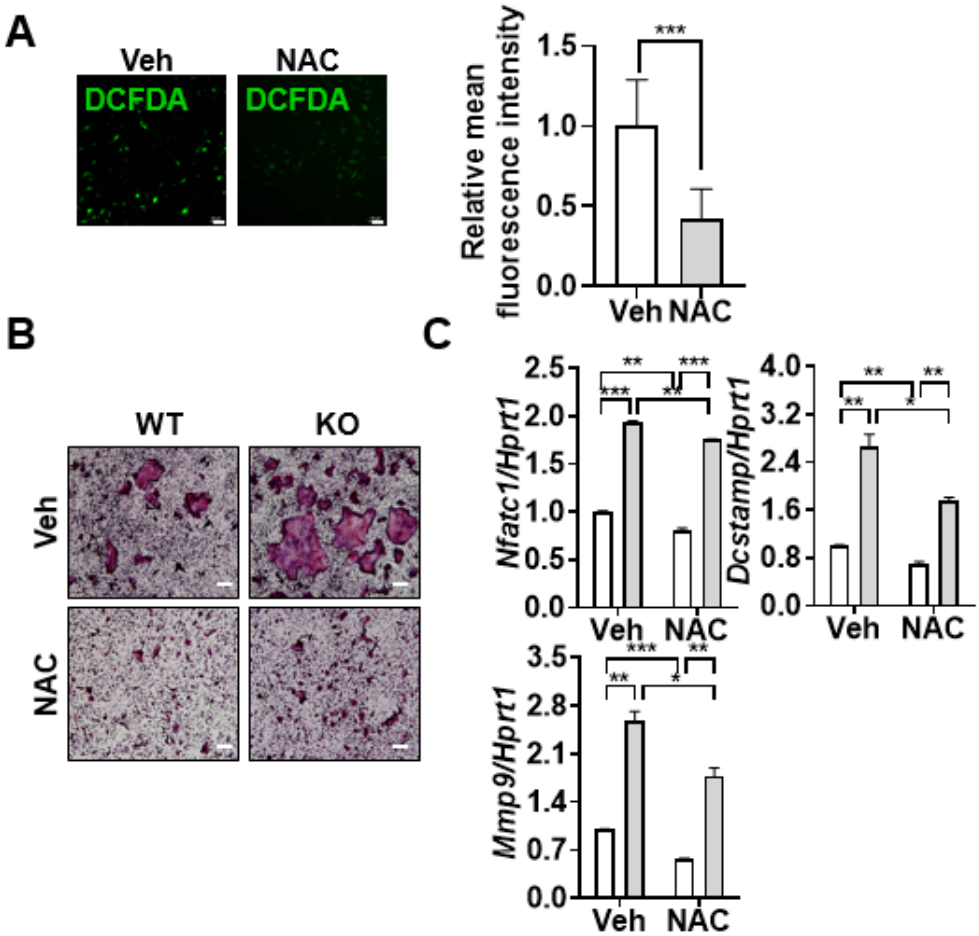

Figure 14. Augmentation of osteoclast differentiation induced by deficiency of PINK1 is partially dependent on ROS accumulation. (A) BMMs treated with vehicle (Veh) or NAC (2.5 mM) were cultured for 2 days and were subjected to confocal analysis for intracellular ROS. *** $P < 0.001$ versus Veh treated group. Scale bars, 50 μm. (B) WT or KO BMMs were cultured with RANKL and M-CSF for 3 days in the presence of Veh or NAC (2.5 mM) and then stained for TRAP. Scale bars, 200 μm. (C) BMMs harvested from either WT or *Pink1* KO mouse were cultured with the

osteoclastogenic medium in the presence of Veh or NAC (2.5 mM) for 2 days. The mRNA levels of osteoclast marker genes were analyzed by real-time PCR. * $P < 0.05$, ** $P < 0.01$, *** $P < 0.001$.

3.6. PINK1 deficiency shows no effects on apoptosis and adenosine triphosphate (ATP) shortage during osteoclast differentiation

Mitochondrial dysfunction can lead to apoptosis (Eckert et al. 2003). Mitochondrial translocation of BAX, a pro-apoptotic member of the Bcl-2 protein family, is a defining feature of apoptosis in mammalian cells (Lindsay et al. 2011). Therefore, I examined whether PINK1 deficiency might change the mitochondrial level of BAX. PINK1 deficiency showed no effects on mitochondrial BAX levels as well as localization of BAX in mitochondria (Figure 15A-B). Also, FACS analyses of cells stained with PI and AnnexinV showed no difference between WT and *Pink1* KO pOCs (Figure 15C). These data suggest that PINK1 has no significant roles in mitochondria-dependent apoptosis in osteoclasts.

It has been reported that PINK1 regulates mitochondrial ATP synthesis through phosphorylation of complex I accessory protein, NDUFA10 (Morais et al. 2014; Pogson et al. 2014). Mitochondrial ETC complex changes affect oxidative phosphorylation and alter cellular metabolism (Zhao et al. 2019). Interestingly, there was no significant difference in ATP production between *Pink1* KO and the WT pOCs (Figure 16A). However, an increase in lactate production was observed in *Pink1* KO pOCs (Figure 16B). These results

suggest that PINK1 deficiency during osteoclast differentiation has little effects on mitochondrial damage-related ATP deficiency.

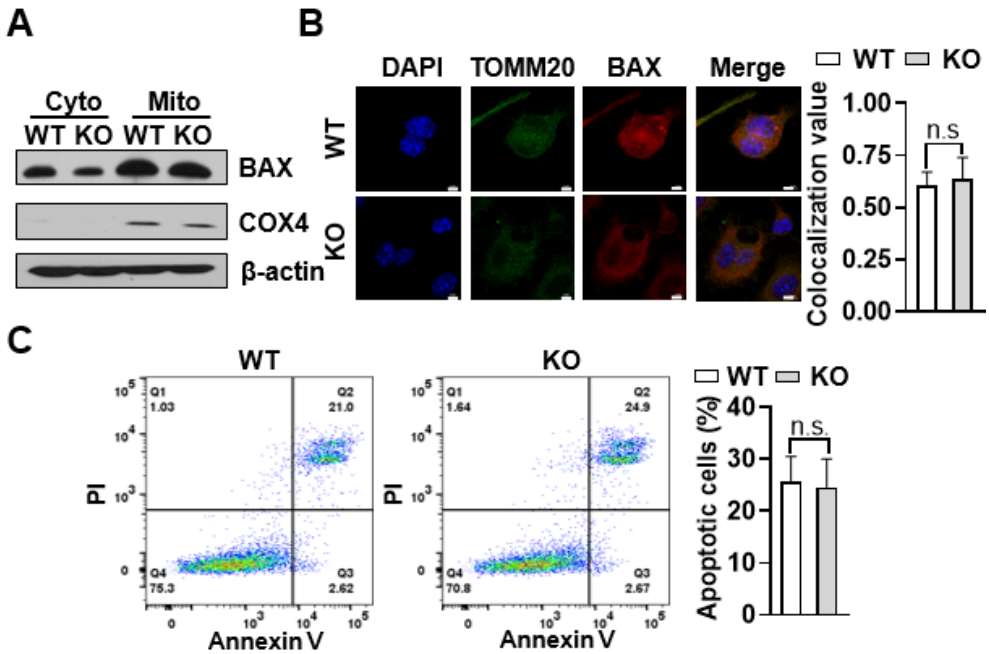

Figure 15. PINK1 deficiency shows no effects on the apoptosis of pOCs. (A) Mitochondria prepared from WT and KO pOCs were subjected to western blotting. Cyto, Cytosol; Mito, Mitochondria. (B) WT and KO pOCs were fixed, permeabilized, blocked, then incubated with BAX antibody (1:200) and TOMM20 antibody (1:200) at 4°C overnight. After washing cells, fluorochrome-conjugated secondary antibody (1:200) was incubated with cells for 1 h in the dark. DAPI was counterstained to indicate the nucleus. The images were acquired with a confocal microscope. Scale bars, 5 μm. (C) WT or *Pink1* KO BMMs were cultured in the presence of M-CSF (30 ng/ml) and RANKL (100 ng/ml) for 2 days and were subjected to FACS analysis. Annexin V/PI staining was performed for the detection of apoptosis.

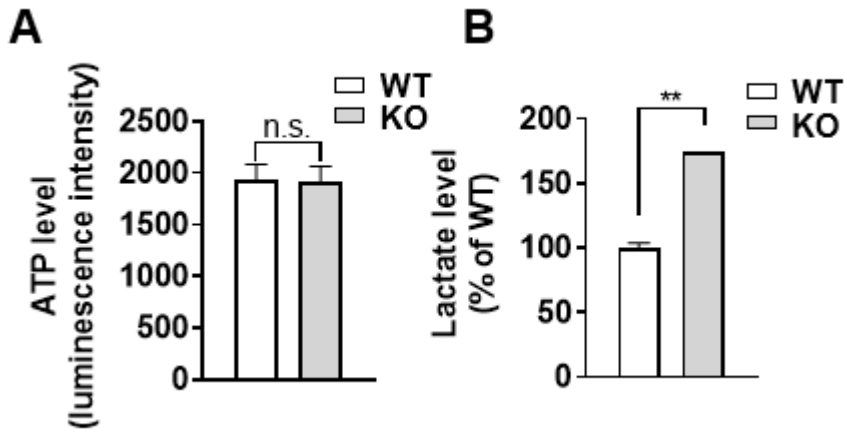

Figure 16. Evaluation of the ATP and lactate levels in WT and KO pOCs. (A) BMMs isolated from WT or *Pink1* KO mice were seeded in 96-well plate and were cultured with the osteoclastogenic medium for 2 days. The end product of mitochondrial respiration was measured by detecting luminescence. (B) WT and *Pink1* KO BMMs were seeded in 6-well plate and cultured in the osteoclastogenic medium for 2 days. Intracellular lactate level of each group was measured by using the colorimetric/fluorometric assay kit. ** $P < 0.01$ versus WT.

3.7. Loss of PINK1 impairs mitophagy during osteoclast differentiation

The term "mitophagy" is used to describe one of the mitochondrial quality control mechanisms that preserve cellular homeostasis by selectively eliminating dysfunctional mitochondria (Goiran et al. 2022). Recent findings show that the occurrence of red mt-Keima punta, indicative of mitophagy, decreased in *Pink1* knock-downed pre-osteoblastic cells (Lee et al. 2021). To determine the occurrence of mitophagy in RANKL-induced osteoclastogenesis, I first evaluated the co-localization of autophagy marker with Mitotracker in BMMs after treatment with or without RANKL. The abundance of co-localization between the two markers was very low in BMMs but strongly elevated in pOCs, suggesting that mitophagy might has functional role in osteoclasts (Figure 17).

To gain insights on the role of PINK1 regulation of mitophagy in osteoclastogenesis, I performed quantum RNA sequencing of pOCs from WT and KO mice. GO analysis of the obtained data revealed that genses involved in macromitophagy were differentially expressed (Figure 18). Next, I examined the level of LC3 protein in mitochondria by immunoblotting and immunofluorescence analyses. Immunoblotting showed that the expression of LC3 protein from each mitochondrial compartment was markedly

suppressed with the loss of PINK1 (Figure 19A). In addition, PINK1 KO pOCs showed lower intensity of LC3B–positive puncta compared to WT pOCs as well as reduced localization of LC3B in mitochondria (Figure 19B). To further investigate whether autophagic flux is altered in *Pink1* KO pOCs, I treated bafilomycin A1, which inhibits autophagosome-lysosome fusion by inhibiting vacuolar H^+-ATPase (Mauvezin and Neufeld 2015). The LC3 II/I ratio, an indicative of autophagic flux, was also slightly reduced in KO group upon treatment of bafilomycin A1, suggesting that loss of PINK1 suppresses autophagolysosome formation (Figure 20A). Similar results were obtained in *Pink1* KO pOCs transfected with tandem-tagged RFP-GFP-LC3, which displays yellow fluorescence in autophagosomes, whereas GFP fluorescence is quenched under acidic lysosomal conditions (Figure 20B). Altogether, these data indicate that PINK1 deficiency led to mitophagy suppression in pOCs.

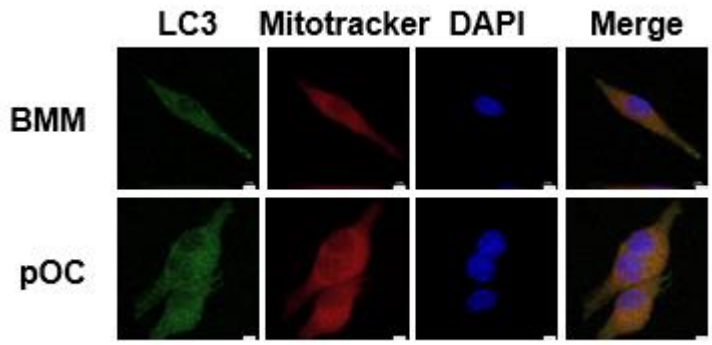

Figure 17. Verification of the mitophagy induction during osteoclast differentiation. Cells were plated onto a cover glass and then incubated with Mitotracker for 45 min. After fixing, cells were incubated with antibody specific to LC3 for overnight and then incubated with secondary antibody. Nuclei were stained with DAPI. Representative images of autophagy marker colocalized with mitochondria during osteoclast formation were obtained by confocal microscopy. Scale bars, 5 μm.

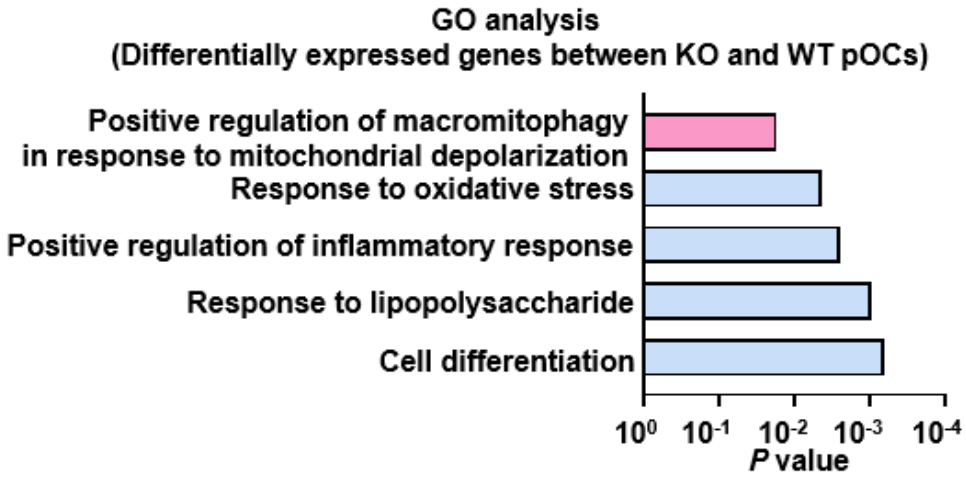

Figure 18. GO analysis of quantum RNA sequencing data. The genes corresponding to logFC > 2 and *P* value < 0.05 were used for GO analysis with the DAVID 6.7 software. The length of the bar represents the -log 10-transformed *P* value.

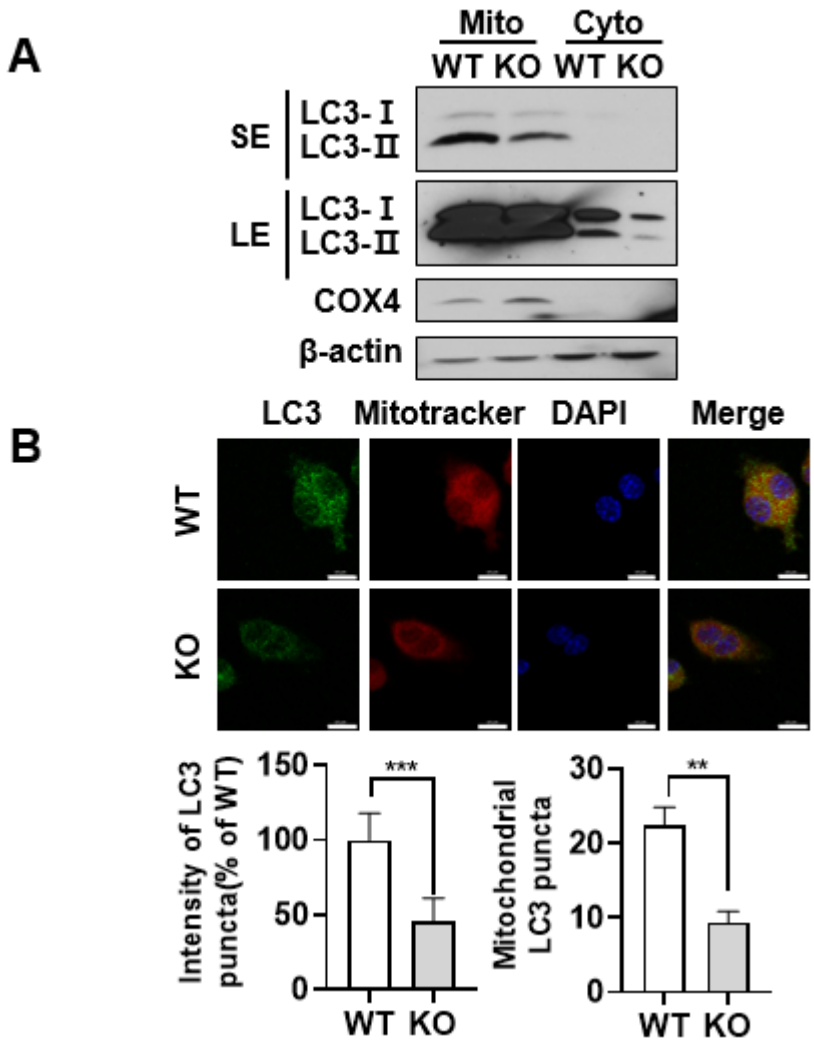

Figure 19. Confirmation of mitophagy by western blotting and immunofluorescence analyses. (A) Mitochondria harvested from WT and KO pOCs were subjected to western blotting. Mito, Mitochondria; Cyto, Cytosol; SE, Short Exposure; LE, Long Exposure. (B) WT and KO pOCs were stained with LC3 antibody and Mitotracker and then were subjected to confocal microscopy. Scale bars, 10 μm.

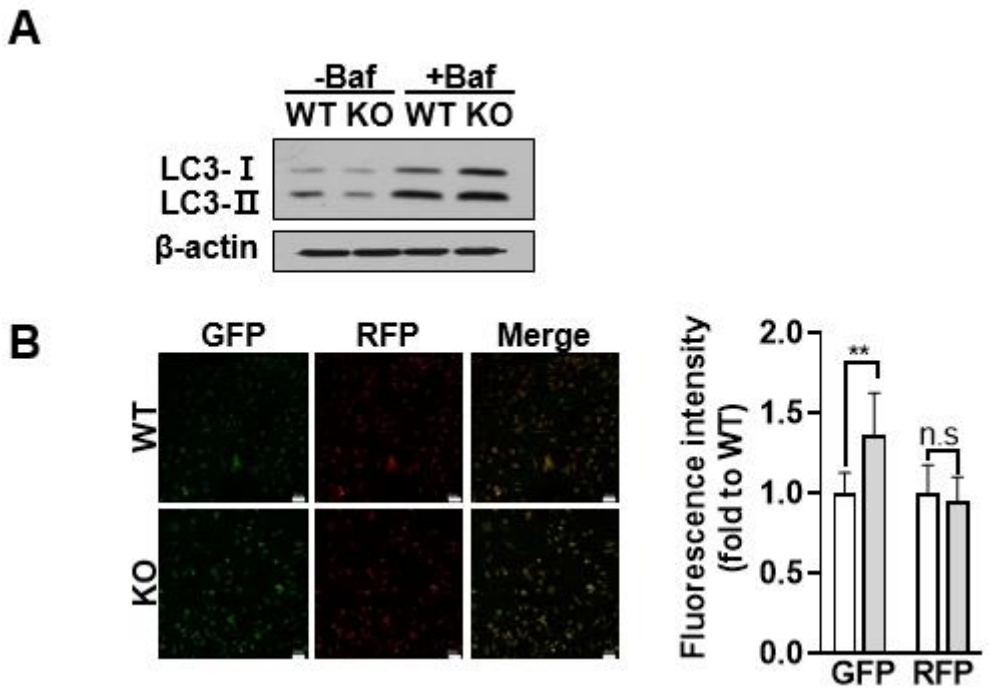

Figure 20. PINK1 deficiency impairs mitophagic functions in pOCs. (A) BMMs derived from WT and KO mice were cultured in the osteoclastogenic medium for 2 days and then treated with bafilomycin A1 (Baf, 50 nM) for 4 h. Cell lysate was prepared and western blotting was performed. (B) WT and KO BMMs were transfected with GFP-RFP-LC3 plasmid and then further cultured with M-CSF (30 ng/ml) and RANKL (100 ng/ml) for 2 days for confocal microscopy. Scale bars, 50 μm.

3.8. Restoration of mitophagy alleviates mitochondrial degeneracy and excessive osteoclast differentiation induced by PINK1 deficiency

SPD is a natural polyamine that promotes auto/mitophagy (D'Adamo et al. 2020; Srivastava et al. 2022) and inhibits osteoclast differentiation (Yamamoto et al. 2012). However, its potential inhibitory effects on osteoclasts differentiation due to autophagy induction has not yet been investigated. To address this, at first, I applied SPD during osteoclast differentiation. SPD show an increase in the mitochondrial staining of LC3 protein (Figure 21). Furthermore, SPD treatment suppressed osteoclast differentiation (Figure 22A), and downregulated the expression of c-Fos and NFATc1 proteins (Figure 22B) and key osteoclastogenic marker genes (Figure 22C). Additionally, to exclude the possibility that the observed inhibitory effect of SPD on osteoclastogenesis might be due to cytotoxicity, a cytotoxicity assay was performed. I found that SPD has no cytotoxic effect on BMMs at the concentrations used in this study (Figure 23).

I hypothesized that inducing mitophagy by SPD treatment can improve impaired mitochondrial function and can inhibit aberrant osteoclast formation caused by genetic ablation of *Pink1*. As a result, addition of SPD blunted the increase in multinuclear $TRAP^+$ cell formation (Figure 24A),

mitigated NFATc1 phosphorylation (Figure 24B) and reduced the transcriptional expression of *Nfatc1* downstream molecules (Figure 24C) under PINK1 depleted conditions. Exogenous supply of SPD for 2 days, significantly reduced mitochondrial and intracellular ROS (Figure 25A) as well as cytosolic Ca^{2+} levels (Figure 25B) in KO pOCs compared to WT pOCs. Collectively, the mitochondrial degeneracy and excessive osteoclast differentiation caused by depletion of PINK1 was alleviated by restoration of mitophagy by SPD treatment.

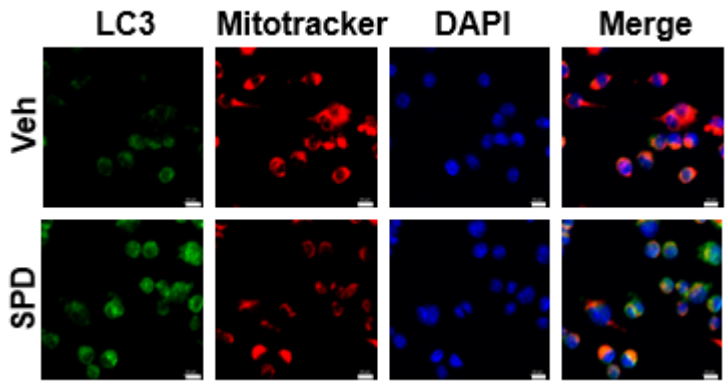

Figure 21. SPD treatment induces mitophagy. BMMs seeded onto a cover glass were treated with 5 μM SPD and cultured with the osteoclastogenic medium for 2 days. Cells were incubated with Mitotracker for 45 min, fixed, and incubated with LC3 antibody. The nuclei were counterstained with DAPI. Representative images of autophagy marker colocalized with mitochondria were obtained by confocal microscopy. Scale bars, 10 μm.

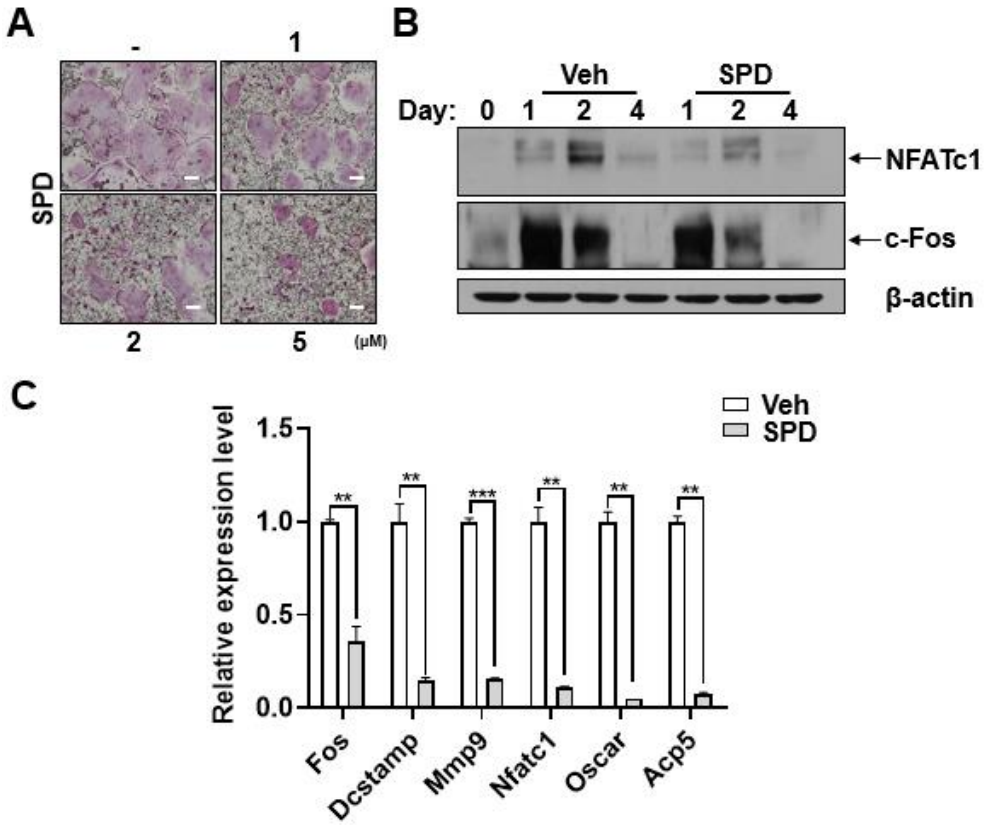

Figure 22. SPD treatment inhibits osteoclast differentiation. (A) After treating with indicated concentrations of SPD in the presence M-CSF+RANKL, the cells were stained for TRAP. Scale bars, 200 μm. (B) BMMs were cultured with Veh or SPD (5 μM) in the presence of M-CSF (30 ng/ml) and RANKL (100 ng/ml). Proteins were prepared from cells harvested at the indicated times and were subjected to western blotting. β-actin was used as an endogenous control. (C) After cells were treated with SPD (5 μM) in the presence M-CSF+RANKL, RNA was prepared and analyzed by real-time PCR. The expression of *Hprt1* was used as an endogenous control. ** $P <$

0.01, *** $P < 0.001$ versus Veh.

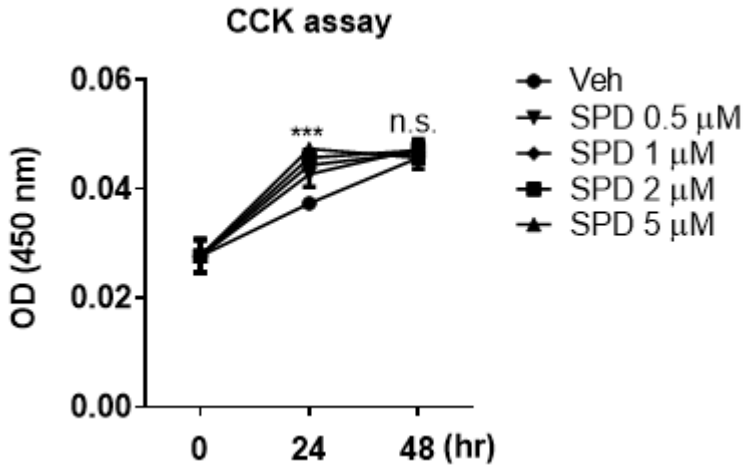

Figure 23. Effect of SPD on the viability of BMMs. The cytotoxic effect of SPD was evaluated using the CCK kit. $1x10^4$ cells were cultured in the presence or absence of various concentrations of SPD for indicated times. Optical density was measured at 450 nm. *** $P < 0.001$ versus Veh. OD, Optical Density.

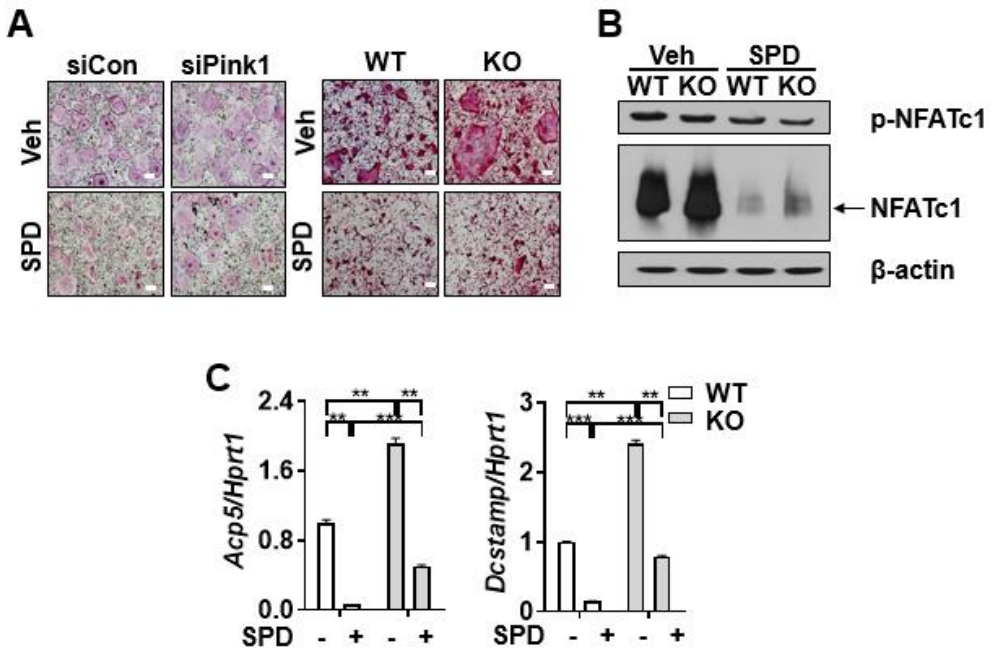

Figure 24. SPD treatment diminishes osteoclast differentiation under PINK1 deficient conditions by blunting the NFATc1 pathway. (A) After culturing BMMs obtained from WT and KO mice with SPD in the presence of MCSF+RANKL, the osteoclast differentiation was assessed by TRAP staining. Scale bars, 200 μm. (B) Cells treated with SPD in the presence of MCSF+RANKL were subjected to western blotting. (C) After culturing WT and KO-derived BMMs with SPD in the osteoclastogenic medium, the expression level of *Acp5* and *Dcstamp* were assessed by real-time PCR. *Hprt1* was used as an endogenous mRNA control in real-time PCR. ** $P < 0.01$, *** $P < 0.001$.

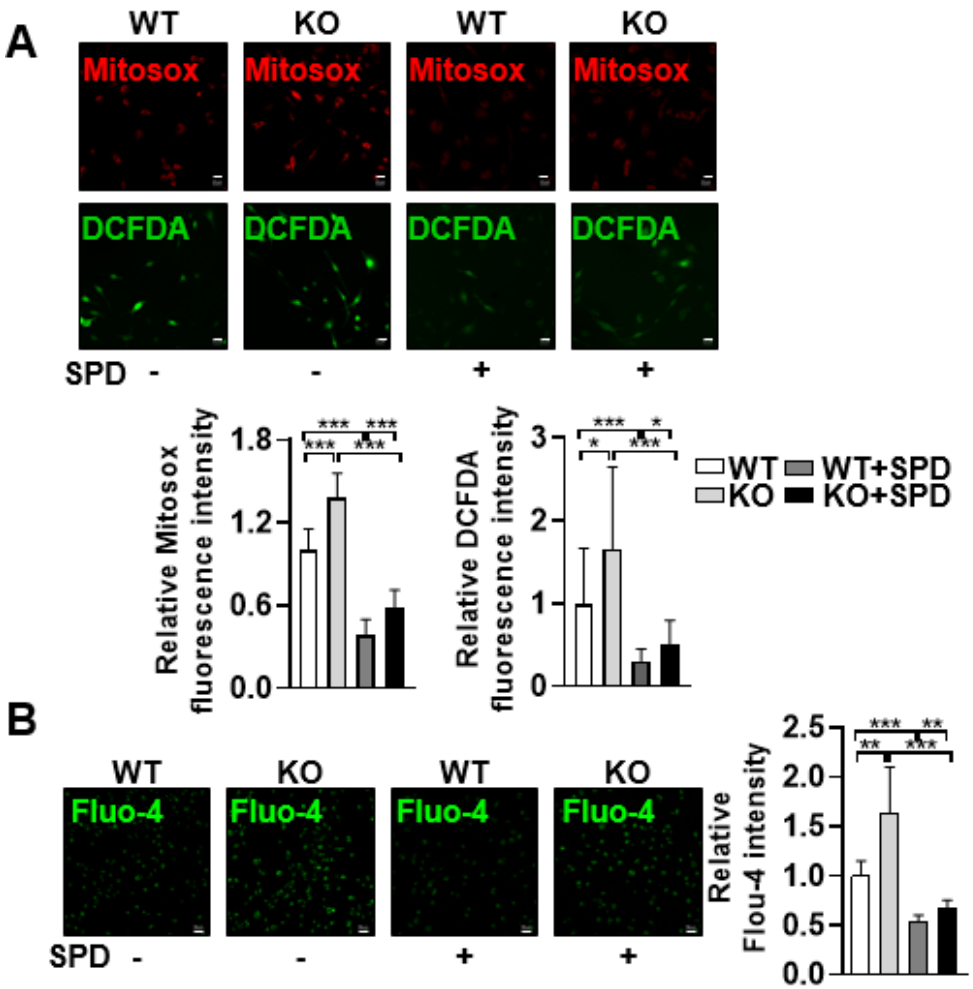

Figure 25. SPD treatment relieves mitochondrial dysfunction under PINK1 deficient conditions. (A) WT and KO BMMs were cultured with 5 μM SPD in the osteoclastogenic medium for 2 days and then were subjected to the measurements of mitochondrial and intracellular ROS. * $P < 0.05$, ** $P < 0.01$, *** $P < 0.001$. (B) WT and KO BMMs were cultured with SPD in the osteoclastogenic medium for 2 days and then cytosolic Ca^{2+} level was measured by a confocal microscope. Relative fluorescence intensity of Flou-

4 was analyzed with the LSM Browser software.

3.9. Genetic ablation of *Pink1* exacerbates alveolar bone loss in mice

Dysregulation of mitochondria and ROS production are usually found as hallmarks in periodontitis patients (Liu et al. 2022). Given that PINK1 is responsible for mitochondrial function and its quality control (Deas et al. 2009; Gautier et al. 2008; Sandebring et al. 2009), PINK1 may have a role in maintaining periodontal health. To investigate the role of PINK1 in inflammatory periodontitis, I utilized a LIP model in 11-week-old WT and *Pink1* KO mice. Both the WT-LIP and KO-LIP groups showed severe periodontitis upon ligature placement. However, more alveolar bone loss was found in the KO-LIP group than in the WT, as indicated by μCT analysis of bone volume fraction and trabecular thickness (Figure 26). Next, I measured the number of osteoclasts in inter-radicular septum area of maxillary second molar through TRAP staining. Consistently, an increase in the number of $TRAP^+$ cells on the alveolar bone surface was observed in both WT- and KO-LIP groups, but showed a more severe increase in the KO-LIP group than in the WT-LIP group (Figure 27). Taken together, these results indicate that PINK1 may have a role in protecting alveolar bone loss from experimental periodontitis.

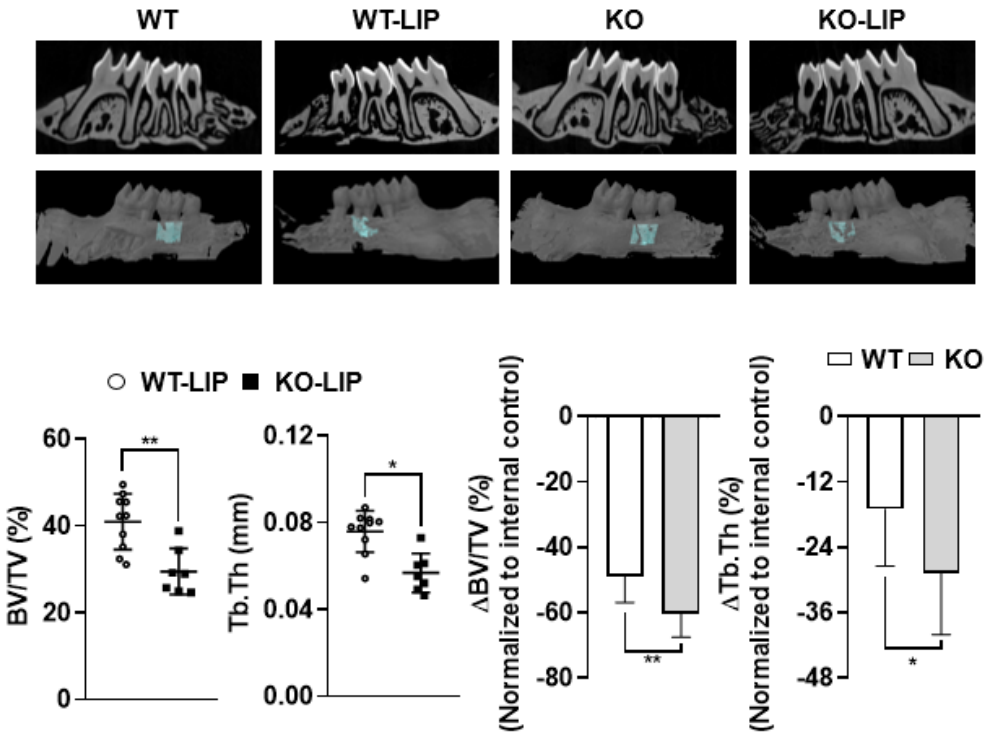

Figure 26. PINK1 deficiency aggravates periodontitis. Alveolar bone was analyzed by μCT. More reduction in bone volume/total volume (BV/TV) and trabecular thickness (Tb.Th) ratio was observed in *Pink1* KO-LIP mice than in WT-LIP mice. * $P < 0.05$, ** $P < 0.01$.

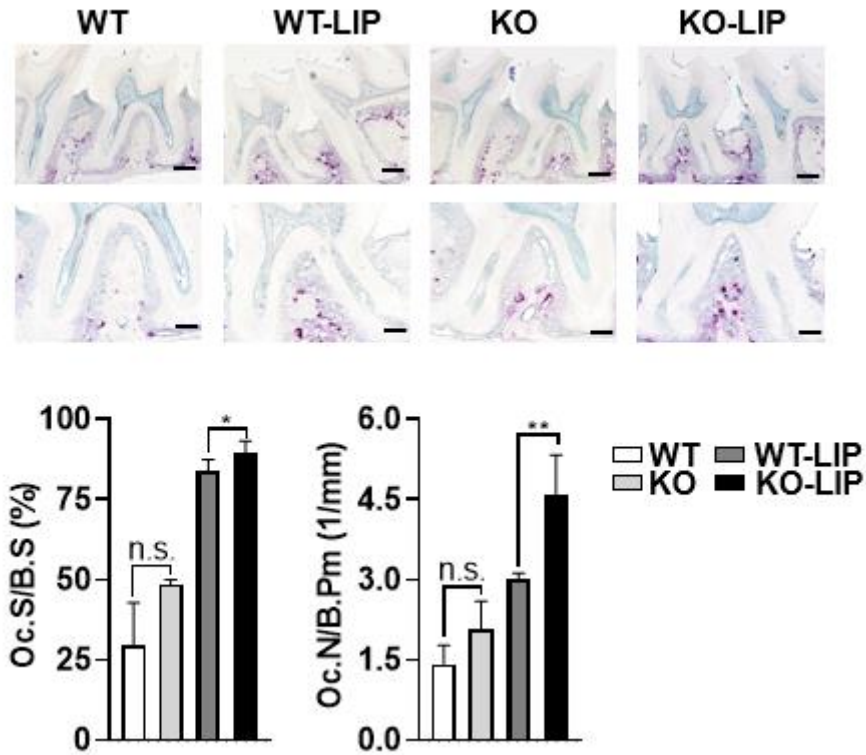

Figure 27. Histological evaluation of periodontal tissues by TRAP staining. Representative TRAP staining image of periodontal tissues. Scale bars, 200 μm and 100 μm for upper and lower pannels, respectively. Significantly increased osteoclast surface/bone surface (Oc.S/B.S) and osteoclast number/bone perimeter (Oc.N/B.Pm) were observed in periodontitis-induced *Pink1* KO than in WT mice. * $P < 0.05$, ** $P < 0.01$.

IV. Discussion

Maintaining mitochondrial functional homeostasis is essential to suppress abnormal osteoclast formation and periodontal deterioration (Angireddy et al. 2019). Mitophagy, a mitochondrial quality control mechanism, may prevent age-related diseases (Bakula and Scheibye-Knudsen 2020; Chen et al. 2020) by mitigating increased Ca^{2+} release and ROS production by damaged mitochondria (Drago et al. 2011; Peng and Jou 2010). However, the essential function of PINK1, a well-known mitophagy inducer, for osteoclast differentiation and bone resorption is still lacking. Here, I revealed that PINK1 deficiency decreased bone mass and increased osteoclast number and activity in *Pink1* KO mice with LIP (Figures 26-27). A series of *in vitro* studies have shown that PINK1 deficiency-induced mitochondrial defects (Figures 12-13) are accompanied by increased intracellular Ca^{2+} level (Figure 10A), unusual nuclear translocation of NFATc1 (Figure 10C), and enhanced ROS production (Figure 13B), which increased the preference for osteoclast differentiation (Figures 4-9). When *Pink1* is genetically depleted, mitophagy number and activity are reduced in pOCs (Figures 19-20). On the other hand, enhanced osteoclast differentiation and mitochondrial damage resulting from the genetic ablation of *Pink1* are partially restored by the induction of mitophagy through SPD treatment (Figures 24-25). Collectively, these data suggest that PINK1 plays a distinct

role in maintaining the mitochondrial function, limiting abnormal osteoclast formation, and consequently maintaining intact periodontal health (Figure 28).

PINK1 is a serine/threonine kinase identified as a causative gene in Parkinson's disease and is implicated in several cellular processes (Vazquez-Martin et al. 2016; Voigt et al. 2016; Wang et al. 2021; Xiong et al. 2009). PINK1 is a mitochondrial kinase involved in mitochondrial quality control and the promotion of cell survival (Matsuda et al. 2013). Defective mitochondria can be detrimental to cellular homeostasis, so quality control mechanisms such as PINK1-mediated mitophagy are essential to restore and conserve energy metabolism. PINK1 is not only associated with mitophagy but also with other mitochondrial quality control, including mitochondrial dynamics through dynamin-associated protein 1 (Yang et al. 2008) and mitochondria-derived vesicles (Mouton-Liger et al. 2017) to maintain mitochondrial homeostasis. Therefore, the constant expression of PINK1 is thought to play a crucial role in cellular homeostasis. Regulation of *PINK1* gene expression has not yet been well addressed. However, the recent studies revealed that several putative transcription factor-binding elements, such as activating transcription factor 3 (Bueno et al. 2018), and nuclear factor kappa-light-chain-enhancer of activated B cells (NFκB) (Duan et al. 2014), are contained in the human *PINK1* promoter. In the case of NFκB, luciferase analysis confirmed that the NFκB binding site was directly attached to the

promoter of the human *PINK1* gene. In addition, overexpression of NFκB p65 dramatically increased *PINK1* promoter activity. Consistently, both real-time PCR and western blotting analysis showed significantly increased expressions of *Pink1* level under osteoclast differentiation (Figure 3).

For skeletal physiology, PINK1 has recently been implicated in osteoblast differentiation (Lee et al. 2021). Interestingly, results similar to this study were found during osteoblast differentiation in *Pink1* KO mice, including a decrease in mitochondrial function, metabolic reprogramming towards glycolysis, and defects in impaired mitochondrial clearance (Lee et al. 2021). These points suggest that mitochondria damage caused by PINK1 deficiency has a great effect on bone cell differentiation as in other stem cells.

Impairment of mitochondrial dynamics is often associated with bone loss because osteoclasts consume significant amounts of energy during bone resorption (Da et al. 2021). One way that impaired mitochondrial dynamics is thought to contribute to bone loss is through loss of $\Delta\Psi m$, leading to a decrease in ATP production (Wang et al. 2020). A compensatory response to reduced mitochondrial oxidative metabolism and ATP production initiates a metabolic shift to glycolysis, a major source of ATP that occurs outside the mitochondria (Lopaschuk et al. 2021). Several studies have shown that loss of PINK1 expression triggers metabolic shift into glycolysis in combination with a high maximal glycolytic capacity in other cell types (Requejo-Aguilar

et al. 2014; Yao et al. 2011). In this study, albeit to a lower ΔΨm in *Pink1* KO pOCs (Figure 13A), there was no significant difference in ATP production between WT and *Pink1* KO (Figure 16A), whereas *Pink1* KO pOCs showed a higher lactate production (Figure 16B) with the significant increase in mitochondrial numbers. Similar results were also detected in *pink-1* KO worms with more mitochondria while similar ATP levels were observed compared to WT worms (Cooper et al. 2017). Also, complex IVi1 and Vb subunits-deficient BMMs showed resemblant phenomena to *Pink1* KO pOCs, such as a preference for glycolysis, higher intracellular Ca^{2+} release, and activation of NFATc1 (Angireddy et al. 2019).

Mitochondria are essential organelles for ROS production that contribute to vital cellular functions such as cell proliferation, differentiation, apoptosis, and senescence (Dan Dunn et al. 2015; Zhang et al. 2016). Previous reports suggest that glutathionylation of complex I and a rise in cytosolic Ca^{2+} level can elevate mitochondrial ROS production (Gandhi et al. 2009; Taylor et al. 2003). *Pink1* deficiency or mutation is associated with reduced mitochondrial complex I activity (Pogson et al. 2014) and cytosolic Ca^{2+} extrusion (Heeman et al. 2011), both of which are associated with ROS production. Also, PINK1 has been reported to protect against oxidative stress by phosphorylating heat shock protein 70/ heat shock protein 90 chaperone systems (Pridgeon et al. 2007). Consistent with previous studies, an increase

in cytosolic Ca^{2+} concentration (Figure 10A) with mitochondrial abnormalities (Figure 12) and high ROS levels (Figure 13B) was observed in *Pink1* KO pOCs.

The invasion of pathogenic bacteria causes inflammatory diseases (Chaukimath et al. 2022; Chen et al. 2022; Qin et al. 2022). Cytosolic DNA derived from pathogens or host genome especially mitochondrial DNA activates the innate immune pathways (Patrick et al. 2016). As one trigger of the innate immune system, the cyclic GMP-AMP synthase (cGAS) interacts with mitochondrial DNA that leaked into the cytosol and activates the stimulator of interferon genes (STING) pathway, subsequently inducing the production of type I interferons and inflammatory cytokines (Ou et al. 2021; Zhou et al. 2021). Recently, one research showed that the expression of STING protein was higher in the basal epithelium and the vascular wall of the connective tissue of periodontitis patients compared to healthy controls, indicating the cGAS/STING innate-immune signaling plays a vital role in the periodontitis (Elmanfi et al. 2021). Not only inducing inflammation, the cGAS/STING pathway was also shown to stimulate macrophage phenotype transition to the classically activated (M1) (Wu et al. 2022). Although both M1 and alternatively activated (M2) macrophages accumulate in periodontal lesions, the transformation of M2 to M1 macrophages is crucial for mediating alveolar bone loss (Yang et al. 2018; Yu et al. 2016). Sliter et al. showed that

the lack of PINK1 exhibits mitochondrial dysfunction with mitochondrial DNA leakage into cytosol, triggering activation of the cGAS/STING pathway in various inflammation conditions (Sliter et al. 2018). Consistently, I found accumulation of damaged mitochondria in *Pink1* KO pOCs (Figures 12-13). Moreover, in mouse LIP models, *Pink1* KO mice exhibited alveolar bone loss more severe compared to WT mice (Figure 26). It cannot be ruled out the deleterious effect of the genetic deletion of *Pink1* on periodontitis via M1 polarization through the cGAS-STING pathway, for which further studies are needed.

Periodontitis arises from the interplay between the subgingival dysbiotic microbial community and innate-adaptive immunity (Becerra-Ruiz et al. 2022). As an innate immunity, neutrophils are activated by the dysbiotic microbiota, primarily through complement activation products like complement component 5a. Activated neutrophils not only directly induce tissue damage by inducing ROS and matrix metalloproteinases, but also interact with adaptive immune cells such as B cells, plasma cells, and T helper 17 cells (Huang et al. 2021). Additionally, interactions between adaptive immunity and neutrophils contribute to the production of pro-inflammatory mediators such as interleukin 17 that stimulate osteoclastogenesis (Feng et al. 2022). Furthermore, interleukin 17 has been associated with inflammatory periodontal bone loss and severity of periodontitis (Allam et al. 2011; Eskan

et al. 2012; Ohyama et al. 2009). Therefore, directly reducing cytokines or indirectly suppressing the activity of immune cells that produce inflammatory cytokines is important for treating periodontitis. PINK1 has an impact on the inflammatory response. PINK1 deficiency induces mitophagy defects, increased mitochondrial ROS production, and NLR family pyrin domain containing 3 inflammasome activation, leading to a significant increase in pro-inflammatory cytokine levels (Mouton-Liger et al. 2018; Xu et al. 2020). Additionally, in 2015, a patent (application number: US14/948,095) indicated that treatment with PINK1 protein in a model of rheumatoid arthritis inhibited T helper 17 activity and promotes regulatory T cell activity. Consistently, RNA-seq results of *Pink1* WT and KO pOCs showed significantly different expressions of genes involved in the GO term "positive regulation of inflammatory response" (Figure 18). Since I induced periodontitis in general KO mice, I cannot rule out the role of PINK1 in regulating the inflammatory response to periodontal bone loss.

Autophagy is a highly conserved intracellular vacuolar process for the degradation of misfolded proteins and damaged organelle, thereby protecting against cell damage and elevating survival (Das et al. 2012; Glick et al. 2010). Mitophagy, a form of selective autophagy, plays an essential role in mitochondrial quality control (Ma et al. 2020). Although the role of autophagy in the regulation of osteoclasts has been reported (Montaseri et al.

2020; Xiao and Xiao 2019), the function of mitophagy in osteoclast formation has been rarely studied. In case of autophagy, it has been reported to play dual roles in osteoclast regulation (Montaseri et al. 2020; Xiao and Xiao 2019). For example, genetic depletion of genes involved in autophagosome formation (*Atg5* and *Atg7*) in BMMs shows a decrease in resorption activity without affecting osteoclast differentiation (DeSelm et al. 2011; Jaber et al. 2019). In contrast, Li et al. reported a significantly lower trabecular bone volume with increased osteoclast bone resorption in osteoblast-specific *Atg7* conditional-KO mice than in WT mice (Li et al. 2018). Interestingly, similar phenomena appear when chemical regulators of autophagy were treated to osteoclasts. Treatment with the autophagy activator (rapamycin) reduced osteoclast formation *in vitro* and prevent bone loss *in vivo* (Owen et al. 2015), but others argues that another autophagy inhibitor (3-methyladenine) attenuated the transient receptor potential vanilloid 4-induced osteoclastogenesis (Cao et al. 2019). Consistent with the negative effects of autophagy on osteoclast formation, in my study, the auto/mitophagy inducer SPD attenuated PINK1-induced osteoclastogenesis (Figure 24). Beyond the induction of auto/mitophagy, SPD also participates in polyamine-associated metabolic pathways and acts as an antioxidant. Therefore, the effects of other autophagy activating agents on PINK1-deficient BMMs remain to be tested.

In conclusion, I demonstrated that the suppression of PINK1 activity

enhances osteoclastogenesis. The reduction in PINK1 expression leads to mitochondrial dysfunction, which turns on the osteoclastogenesis program by activating the NFATc1 pathway. Lack of PINK1 accelerated alveolar bone loss in the LIP model. I also showed that the addition of mitophagy inducer blunts the increase in multinuclear $TRAP^{+}$ cell formation and moderates the increase in mRNA levels of genes that are transcriptionally regulated by the NFATc1 signaling in PINK1-deficient conditions. Taken together, agents activating PINK1 expression or improving damaged mitochondrial functions may have therapeutic potential in bone diseases.

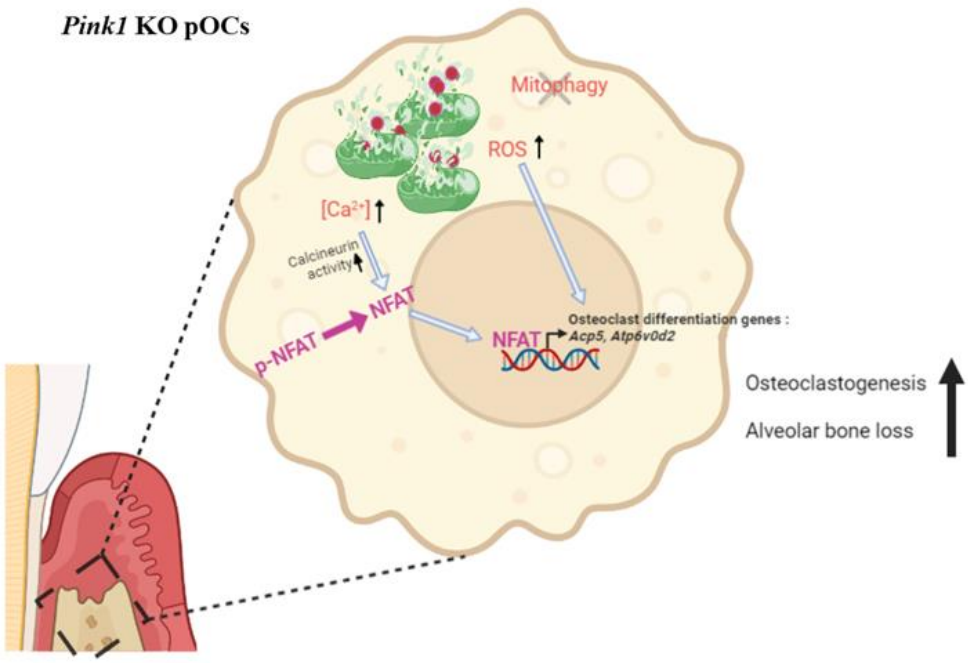

Figure 28. Graphical summary of the effects of PINK1 on osteoclast differentiation. PINK1 deficiency induces excessive osteoclast differentiation as a consequence of mitochondrial dysfunctions, mitophagy impairments, dysregulated reactive oxygen species production, and overactivation of the Ca^{2+}-NFATc1 signaling. Additionally, PINK1 deficiency aggravates the alveolar bone loss in mice with LIP (illustrated by using https://app.biorender.com).

V. References

Allam JP, Duan Y, Heinemann F, Winter J, Gotz W, Deschner J, Wenghoefer M, Bieber T, Jepsen S, Novak N. 2011. Il-23-producing cd68(+) macrophage-like cells predominate within an il-17-polarized infiltrate in chronic periodontitis lesions. J Clin Periodontol. 38(10):879-886.

An D, Kim K, Lu W. 2014. Defective entry into mitosis 1 (dim1) negatively regulates osteoclastogenesis by inhibiting the expression of nuclear factor of activated t-cells, cytoplasmic, calcineurin-dependent 1 (nfatc1). J Biol Chem. 289(35):24366-24373.

Angireddy R, Kazmi HR, Srinivasan S, Sun L, Iqbal J, Fuchs SY, Guha M, Kijima T, Yuen T, Zaidi M et al. 2019. Cytochrome c oxidase dysfunction enhances phagocytic function and osteoclast formation in macrophages. FASEB J. 33(8):9167-9181.

Ashrafi G, Schwarz TL. 2013. The pathways of mitophagy for quality control and clearance of mitochondria. Cell Death Differ. 20(1):31-42.

Bakula D, Scheibye-Knudsen M. 2020. Mitophaging: Mitophagy in aging and disease. Front Cell Dev Biol. 8:239.

Becerra-Ruiz JS, Guerrero-Velazquez C, Martinez-Esquivias F, Martinez-Perez LA, Guzman-Flores JM. 2022. Innate and adaptive immunity of periodontal disease. From etiology to alveolar bone loss. Oral Dis. 28(6):1441-1447.

Beilina A, Van Der Brug M, Ahmad R, Kesavapany S, Miller DW, Petsko GA, Cookson MR. 2005. Mutations in pten-induced putative kinase 1 associated with recessive parkinsonism have differential effects on protein stability. Proc Natl Acad Sci U S A. 102(16):5703-5708.

Bleier L, Drose S. 2013. Superoxide generation by complex iii: From mechanistic rationales to functional consequences. Biochim Biophys Acta. 1827(11-12):1320-1331.

Boyle WJ, Simonet WS, Lacey DL. 2003. Osteoclast differentiation and activation. Nature. 423(6937):337-342.

Bueno M, Brands J, Voltz L, Fiedler K, Mays B, St Croix C, Sembrat J, Mallampalli RK, Rojas M, Mora AL. 2018. Atf3 represses pink1 gene transcription in lung epithelial cells to control mitochondrial homeostasis. Aging Cell. 17(2):e12720.

Bullon P, Cordero MD, Quiles JL, Ramirez-Tortosa Mdel C, Gonzalez-Alonso A, Alfonsi S, Garcia-Marin R, de Miguel M, Battino M. 2012. Autophagy in periodontitis patients and gingival fibroblasts: Unraveling the link between chronic diseases and inflammation. BMC Med. 10:122.

Cairns G, Thumiah-Mootoo M, Burelle Y, Khacho M. 2020. Mitophagy: A new player in stem cell biology. Biology (Basel). 9(12):481.

Cao B, Dai X, Wang W. 2019. Knockdown of trpv4 suppresses osteoclast

differentiation and osteoporosis by inhibiting autophagy through ca(2+) -calcineurin-nfatc1 pathway. J Cell Physiol. 234(5):6831-6841.

Chaukimath P, Frankel G, Visweswariah SS. 2022. The metabolic impact of bacterial infection in the gut. FEBS J. (Online ahead of print).

Chen G, Kroemer G, Kepp O. 2020. Mitophagy: An emerging role in aging and age-associated diseases. Front Cell Dev Biol. 8:200.

Chen X, Wang Z, Duan N, Zhu G, Schwarz EM, Xie C. 2018. Osteoblast-osteoclast interactions. Connect Tissue Res. 59(2):99-107.

Chen Y, Huang Z, Tang Z, Huang Y, Huang M, Liu H, Ziebolz D, Schmalz G, Jia B, Zhao J. 2022. More than just a periodontal pathogen -the research progress on fusobacterium nucleatum. Front Cell Infect Microbiol. 12:815318.

Chen Y, Ji Y, Jin X, Sun X, Zhang X, Chen Y, Shi L, Cheng H, Mao Y, Li X et al. 2019. Mitochondrial abnormalities are involved in periodontal ligament fibroblast apoptosis induced by oxidative stress. Biochem Biophys Res Commun. 509(2):483-490.

Cooper JF, Machiela E, Dues DJ, Spielbauer KK, Senchuk MM, Van Raamsdonk JM. 2017. Activation of the mitochondrial unfolded protein response promotes longevity and dopamine neuron survival in parkinson's disease models. Sci Rep. 7(1):16441.

D'Adamo S, Cetrullo S, Guidotti S, Silvestri Y, Minguzzi M, Santi S, Cattini

L, Filardo G, Flamigni F, Borzi RM. 2020. Spermidine rescues the deregulated autophagic response to oxidative stress of osteoarthritic chondrocytes. Free Radic Biol Med. 153:159-172.

Da W, Tao L, Zhu Y. 2021. The role of osteoclast energy metabolism in the occurrence and development of osteoporosis. Front Endocrinol (Lausanne). 12:675385.

Dan Dunn J, Alvarez LA, Zhang X, Soldati T. 2015. Reactive oxygen species and mitochondria: A nexus of cellular homeostasis. Redox Biol. 6:472-485.

Das G, Shravage BV, Baehrecke EH. 2012. Regulation and function of autophagy during cell survival and cell death. Cold Spring Harb Perspect Biol. 4(6):a008813.

Deas E, Plun-Favreau H, Wood NW. 2009. Pink1 function in health and disease. EMBO Mol Med. 1(3):152-165.

DeSelm CJ, Miller BC, Zou W, Beatty WL, van Meel E, Takahata Y, Klumperman J, Tooze SA, Teitelbaum SL, Virgin HW. 2011. Autophagy proteins regulate the secretory component of osteoclastic bone resorption. Dev Cell. 21(5):966-974.

Dobson PF, Dennis EP, Hipps D, Reeve A, Laude A, Bradshaw C, Stamp C, Smith A, Deehan DJ, Turnbull DM et al. 2020. Mitochondrial dysfunction impairs osteogenesis, increases osteoclast activity, and

accelerates age related bone loss. Sci Rep. 10(1):11643.

Drago I, Pizzo P, Pozzan T. 2011. After half a century mitochondrial calcium in- and efflux machineries reveal themselves. EMBO J. 30(20):4119-4125.

Duan X, Tong J, Xu Q, Wu Y, Cai F, Li T, Song W. 2014. Upregulation of human pink1 gene expression by nfkappab signalling. Mol Brain. 7:57.

Eckert A, Keil U, Marques CA, Bonert A, Frey C, Schussel K, Muller WE. 2003. Mitochondrial dysfunction, apoptotic cell death, and alzheimer's disease. Biochem Pharmacol. 66(8):1627-1634.

Elmanfi S, Yilmaz M, Ong WWS, Yeboah KS, Sintim HO, Gursoy M, Kononen E, Gursoy UK. 2021. Bacterial cyclic dinucleotides and the cgas-cgamp-sting pathway: A role in periodontitis? Pathogens. 10(6):675.

Eskan MA, Jotwani R, Abe T, Chmelar J, Lim JH, Liang S, Ciero PA, Krauss JL, Li F, Rauner M et al. 2012. The leukocyte integrin antagonist del-1 inhibits il-17-mediated inflammatory bone loss. Nat Immunol. 13(5):465-473.

Fan S, Price T, Huang W, Plue M, Warren J, Sundaramoorthy P, Paul B, Feinberg D, MacIver N, Chao N et al. 2020. Pink1-dependent mitophagy regulates the migration and homing of multiple myeloma cells via the mob1b-mediated hippo-yap/taz pathway. Adv Sci

(Weinh). 7(5):1900860.

Feng Y, Chen Z, Tu SQ, Wei JM, Hou YL, Kuang ZL, Kang XN, Ai H. 2022. Role of interleukin-17a in the pathomechanisms of periodontitis and related systemic chronic inflammatory diseases. Front Immunol. 13:862415.

Florencio-Silva R, Sasso GR, Sasso-Cerri E, Simoes MJ, Cerri PS. 2015. Biology of bone tissue: Structure, function, and factors that influence bone cells. Biomed Res Int. 2015:421746.

Gandhi S, Wood-Kaczmar A, Yao Z, Plun-Favreau H, Deas E, Klupsch K, Downward J, Latchman DS, Tabrizi SJ, Wood NW et al. 2009. Pink1-associated parkinson's disease is caused by neuronal vulnerability to calcium-induced cell death. Mol Cell. 33(5):627-638.

Gautier CA, Kitada T, Shen J. 2008. Loss of pink1 causes mitochondrial functional defects and increased sensitivity to oxidative stress. Proc Natl Acad Sci U S A. 105(32):11364-11369.

Gegg ME, Schapira AH. 2011. Pink1-parkin-dependent mitophagy involves ubiquitination of mitofusins 1 and 2: Implications for parkinson disease pathogenesis. Autophagy. 7(2):243-245.

Glick D, Barth S, Macleod KF. 2010. Autophagy: Cellular and molecular mechanisms. J Pathol. 221(1):3-12.

Goiran T, Eldeeb MA, Zorca CE, Fon EA. 2022. Hallmarks and molecular

tools for the study of mitophagy in parkinson's disease. Cells. 11(13):2097.

Graves DT, Li J, Cochran DL. 2011. Inflammation and uncoupling as mechanisms of periodontal bone loss. J Dent Res. 90(2):143-153.

Guha M, Srinivasan S, Koenigstein A, Zaidi M, Avadhani NG. 2016. Enhanced osteoclastogenesis by mitochondrial retrograde signaling through transcriptional activation of the cathepsin k gene. Ann N Y Acad Sci. 1364(1):52-61.

Ha H, Kwak HB, Lee SW, Jin HM, Kim HM, Kim HH, Lee ZH. 2004. Reactive oxygen species mediate rank signaling in osteoclasts. Exp Cell Res. 301(2):119-127.

Heeman B, Van den Haute C, Aelvoet SA, Valsecchi F, Rodenburg RJ, Reumers V, Debyser Z, Callewaert G, Koopman WJ, Willems PH et al. 2011. Depletion of pink1 affects mitochondrial metabolism, calcium homeostasis and energy maintenance. J Cell Sci. 124(Pt 7):1115-1125.

Huang N, Dong H, Luo Y, Shao B. 2021. Th17 cells in periodontitis and its regulation by a20. Front Immunol. 12:742925.

Jaber FA, Khan NM, Ansari MY, Al-Adlaan AA, Hussein NJ, Safadi FF. 2019. Autophagy plays an essential role in bone homeostasis. J Cell Physiol. 234(8):12105-12115.

Jeong S, Seong JH, Kang JH, Lee DS, Yim M. 2021. Dynamin-related protein 1 positively regulates osteoclast differentiation and bone loss. FEBS Lett. 595(1):58-67.

Jung S, Kwon JO, Kim MK, Song MK, Kim B, Lee ZH, Kim HH. 2019. Mitofusin 2, a mitochondria-er tethering protein, facilitates osteoclastogenesis by regulating the calcium-calcineurin-nfatc1 axis. Biochem Biophys Res Commun. 516(1):202-208.

Khacho M, Harris R, Slack RS. 2019. Mitochondria as central regulators of neural stem cell fate and cognitive function. Nat Rev Neurosci. 20(1):34-48.

Kim JH, Kim N. 2014. Regulation of nfatc1 in osteoclast differentiation. J Bone Metab. 21(4):233-241.

Kim JH, Kim N. 2016. Signaling pathways in osteoclast differentiation. Chonnam Med J. 52(1):12-17.

Kim JM, Lin C, Stavre Z, Greenblatt MB, Shim JH. 2020. Osteoblast-osteoclast communication and bone homeostasis. Cells. 9(9):2073.

Koyano F, Okatsu K, Kosako H, Tamura Y, Go E, Kimura M, Kimura Y, Tsuchiya H, Yoshihara H, Hirokawa T et al. 2014. Ubiquitin is phosphorylated by pink1 to activate parkin. Nature. 510(7503):162-166.

Lazarou M, Sliter DA, Kane LA, Sarraf SA, Wang C, Burman JL, Sideris DP,

Fogel AI, Youle RJ. 2015. The ubiquitin kinase pink1 recruits autophagy receptors to induce mitophagy. Nature. 524(7565):309-314.

Lee SY, An HJ, Kim JM, Sung MJ, Kim DK, Kim HK, Oh J, Jeong HY, Lee YH, Yang T et al. 2021. Pink1 deficiency impairs osteoblast differentiation through aberrant mitochondrial homeostasis. Stem Cell Res Ther. 12(1):589.

Li H, Li D, Ma Z, Qian Z, Kang X, Jin X, Li F, Wang X, Chen Q, Sun H et al. 2018. Defective autophagy in osteoblasts induces endoplasmic reticulum stress and causes remarkable bone loss. Autophagy. 14(10):1726-1741.

Lin Q, Chen J, Gu L, Dan X, Zhang C, Yang Y. 2021. New insights into mitophagy and stem cells. Stem Cell Res Ther. 12(1):452.

Lindsay J, Esposti MD, Gilmore AP. 2011. Bcl-2 proteins and mitochondria-specificity in membrane targeting for death. Biochim Biophys Acta. 1813(4):532-539.

Liu J, Wang Y, Shi Q, Wang X, Zou P, Zheng M, Luan Q. 2022. Mitochondrial DNA efflux maintained in gingival fibroblasts of patients with periodontitis through ros/mptp pathway. Oxid Med Cell Longev. 2022:1000213.

Liu W, Le CC, Wang D, Ran D, Wang Y, Zhao H, Gu J, Zou H, Yuan Y, Bian J et al. 2020. Ca(2+)/cam/camk signaling is involved in cadmium-

induced osteoclast differentiation. Toxicology. 441:152520.

Lopaschuk GD, Karwi QG, Tian R, Wende AR, Abel ED. 2021. Cardiac energy metabolism in heart failure. Circ Res. 128(10):1487-1513.

Ma K, Chen G, Li W, Kepp O, Zhu Y, Chen Q. 2020. Mitophagy, mitochondrial homeostasis, and cell fate. Front Cell Dev Biol. 8:467.

Matsuda S, Kitagishi Y, Kobayashi M. 2013. Function and characteristics of pink1 in mitochondria. Oxid Med Cell Longev. 2013:601587.

Mauvezin C, Neufeld TP. 2015. Bafilomycin a1 disrupts autophagic flux by inhibiting both v-atpase-dependent acidification and ca-p60a/serca-dependent autophagosome-lysosome fusion. Autophagy. 11(8):1437-1438.

Mohanraj K, Nowicka U, Chacinska A. 2020. Mitochondrial control of cellular protein homeostasis. Biochem J. 477(16):3033-3054.

Montaseri A, Giampietri C, Rossi M, Riccioli A, Del Fattore A, Filippini A. 2020. The role of autophagy in osteoclast differentiation and bone resorption function. Biomolecules. 10(10):1398.

Morais VA, Haddad D, Craessaerts K, De Bock PJ, Swerts J, Vilain S, Aerts L, Overbergh L, Grunewald A, Seibler P et al. 2014. Pink1 loss-of-function mutations affect mitochondrial complex i activity via ndufa10 ubiquinone uncoupling. Science. 344(6180):203-207.

Mouton-Liger F, Jacoupy M, Corvol JC, Corti O. 2017. Pink1/parkin-

dependent mitochondrial surveillance: From pleiotropy to parkinson's disease. Front Mol Neurosci. 10:120.

Mouton-Liger F, Rosazza T, Sepulveda-Diaz J, Ieang A, Hassoun SM, Claire E, Mangone G, Brice A, Michel PP, Corvol JC et al. 2018. Parkin deficiency modulates nlrp3 inflammasome activation by attenuating an a20-dependent negative feedback loop. Glia. 66(8):1736-1751.

Negishi-Koga T, Takayanagi H. 2009. Ca2+-nfatc1 signaling is an essential axis of osteoclast differentiation. Immunol Rev. 231(1):241-256.

Ohyama H, Kato-Kogoe N, Kuhara A, Nishimura F, Nakasho K, Yamanegi K, Yamada N, Hata M, Yamane J, Terada N. 2009. The involvement of il-23 and the th17 pathway in periodontitis. J Dent Res. 88(7):633-638.

Okatsu K, Koyano F, Kimura M, Kosako H, Saeki Y, Tanaka K, Matsuda N. 2015. Phosphorylated ubiquitin chain is the genuine parkin receptor. J Cell Biol. 209(1):111-128.

Ou L, Zhang A, Cheng Y, Chen Y. 2021. The cgas-sting pathway: A promising immunotherapy target. Front Immunol. 12:795048.

Owen HC, Vanhees I, Gunst J, Van Cromphaut S, Van den Berghe G. 2015. Critical illness-induced bone loss is related to deficient autophagy and histone hypomethylation. Intensive Care Med Exp. 3(1):52.

Patrick KL, Bell SL, Watson RO. 2016. For better or worse: Cytosolic DNA

sensing during intracellular bacterial infection induces potent innate immune responses. J Mol Biol. 428(17):3372-3386.

Peng TI, Jou MJ. 2010. Oxidative stress caused by mitochondrial calcium overload. Ann N Y Acad Sci. 1201:183-188.

Pogson JH, Ivatt RM, Sanchez-Martinez A, Tufi R, Wilson E, Mortiboys H, Whitworth AJ. 2014. The complex i subunit ndufa10 selectively rescues drosophila pink1 mutants through a mechanism independent of mitophagy. PLoS Genet. 10(11):e1004815.

Pridgeon JW, Olzmann JA, Chin LS, Li L. 2007. Pink1 protects against oxidative stress by phosphorylating mitochondrial chaperone trap1. PLoS Biol. 5(7):e172.

Qin S, Xiao W, Zhou C, Pu Q, Deng X, Lan L, Liang H, Song X, Wu M. 2022. Pseudomonas aeruginosa: Pathogenesis, virulence factors, antibiotic resistance, interaction with host, technology advances and emerging therapeutics. Signal Transduct Target Ther. 7(1):199.

Quinn PMJ, Moreira PI, Ambrosio AF, Alves CH. 2020. Pink1/parkin signalling in neurodegeneration and neuroinflammation. Acta Neuropathol Commun. 8(1):189.

Requejo-Aguilar R, Lopez-Fabuel I, Fernandez E, Martins LM, Almeida A, Bolanos JP. 2014. Pink1 deficiency sustains cell proliferation by reprogramming glucose metabolism through hif1. Nat Commun.

5:4514.

Sandebring A, Thomas KJ, Beilina A, van der Brug M, Cleland MM, Ahmad R, Miller DW, Zambrano I, Cowburn RF, Behbahani H et al. 2009. Mitochondrial alterations in pink1 deficient cells are influenced by calcineurin-dependent dephosphorylation of dynamin-related protein 1. PLoS One. 4(5):e5701.

Seo BJ, Yoon SH, Do JT. 2018. Mitochondrial dynamics in stem cells and differentiation. Int J Mol Sci. 19(12):3893.

Shares BH, Busch M, White N, Shum L, Eliseev RA. 2018. Active mitochondria support osteogenic differentiation by stimulating beta-catenin acetylation. J Biol Chem. 293(41):16019-16027.

Shin HJ, Park H, Shin N, Kwon HH, Yin Y, Hwang JA, Song HJ, Kim J, Kim DW, Beom J. 2019. Pink1-mediated chondrocytic mitophagy contributes to cartilage degeneration in osteoarthritis. J Clin Med. 8(11):1849.

Sima C, Viniegra A, Glogauer M. 2019. Macrophage immunomodulation in chronic osteolytic diseases-the case of periodontitis. J Leukoc Biol. 105(3):473-487.

Sivandzade F, Bhalerao A, Cucullo L. 2019. Analysis of the mitochondrial membrane potential using the cationic jc-1 dye as a sensitive fluorescent probe. Bio Protoc. 9(1):e3128.

Sliter DA, Martinez J, Hao L, Chen X, Sun N, Fischer TD, Burman JL, Li Y, Zhang Z, Narendra DP et al. 2018. Parkin and pink1 mitigate sting-induced inflammation. Nature. 561(7722):258-262.

Soysa NS, Alles N, Aoki K, Ohya K. 2012. Osteoclast formation and differentiation: An overview. J Med Dent Sci. 59(3):65-74.

Srinivasan S, Koenigstein A, Joseph J, Sun L, Kalyanaraman B, Zaidi M, Avadhani NG. 2010. Role of mitochondrial reactive oxygen species in osteoclast differentiation. Ann N Y Acad Sci. 1192:245-252.

Srivastava V, Zelmanovich V, Shukla V, Abergel R, Cohen I, Ben-Sasson SA, Gross E. 2022. Distinct designer diamines promote mitophagy, and thereby enhance healthspan in c. Elegans and protect human cells against oxidative damage. Autophagy.1-31 (Epub ahead of print).

Tanaka A, Cleland MM, Xu S, Narendra DP, Suen DF, Karbowski M, Youle RJ. 2010. Proteasome and p97 mediate mitophagy and degradation of mitofusins induced by parkin. J Cell Biol. 191(7):1367-1380.

Taylor ER, Hurrell F, Shannon RJ, Lin TK, Hirst J, Murphy MP. 2003. Reversible glutathionylation of complex i increases mitochondrial superoxide formation. J Biol Chem. 278(22):19603-19610.

Vazquez-Martin A, Van den Haute C, Cufi S, Corominas-Faja B, Cuyas E, Lopez-Bonet E, Rodriguez-Gallego E, Fernandez-Arroyo S, Joven J, Baekelandt V et al. 2016. Mitophagy-driven mitochondrial

rejuvenation regulates stem cell fate. Aging (Albany NY). 8(7):1330-1352.

Voigt A, Berlemann LA, Winklhofer KF. 2016. The mitochondrial kinase pink1: Functions beyond mitophagy. J Neurochem. 139 Suppl 1:232-239.

Wang C, Liu K, Cao J, Wang L, Zhao Q, Li Z, Zhang H, Chen Q, Zhao T. 2021. Pink1-mediated mitophagy maintains pluripotency through optineurin. Cell Prolif. 54(5):e13034.

Wang S, Deng Z, Ma Y, Jin J, Qi F, Li S, Liu C, Lyu FJ, Zheng Q. 2020. The role of autophagy and mitophagy in bone metabolic disorders. Int J Biol Sci. 16(14):2675-2691.

Wang X, Winter D, Ashrafi G, Schlehe J, Wong YL, Selkoe D, Rice S, Steen J, LaVoie MJ, Schwarz TL. 2011. Pink1 and parkin target miro for phosphorylation and degradation to arrest mitochondrial motility. Cell. 147(4):893-906.

Wauer T, Simicek M, Schubert A, Komander D. 2015. Mechanism of phospho-ubiquitin-induced parkin activation. Nature. 524(7565):370-374.

Wu W, Zhang X, Wang S, Li T, Hao Q, Li S, Yao W, Sun R. 2022. Pharmacological inhibition of the cgas-sting signaling pathway suppresses microglial m1-polarization in the spinal cord and

attenuates neuropathic pain. Neuropharmacology. 217:109206.

Xiao B, Kuruvilla J, Tan EK. 2022. Mitophagy and reactive oxygen species interplay in parkinson's disease. NPJ Parkinsons Dis. 8(1):135.

Xiao L, Xiao Y. 2019. The autophagy in osteoimmonology: Self-eating, maintenance, and beyond. Front Endocrinol (Lausanne). 10:490.

Xiong H, Wang D, Chen L, Choo YS, Ma H, Tang C, Xia K, Jiang W, Ronai Z, Zhuang X et al. 2009. Parkin, pink1, and dj-1 form a ubiquitin e3 ligase complex promoting unfolded protein degradation. J Clin Invest. 119(3):650-660.

Xu Y, Tang Y, Lu J, Zhang W, Zhu Y, Zhang S, Ma G, Jiang P, Zhang W. 2020. Pink1-mediated mitophagy protects against hepatic ischemia/reperfusion injury by restraining nlrp3 inflammasome activation. Free Radic Biol Med. 160:871-886.

Yamamoto T, Hinoi E, Fujita H, Iezaki T, Takahata Y, Takamori M, Yoneda Y. 2012. The natural polyamines spermidine and spermine prevent bone loss through preferential disruption of osteoclastic activation in ovariectomized mice. Br J Pharmacol. 166(3):1084-1096.

Yang J, Zhu Y, Duan D, Wang P, Xin Y, Bai L, Liu Y, Xu Y. 2018. Enhanced activity of macrophage m1/m2 phenotypes in periodontitis. Arch Oral Biol. 96:234-242.

Yang Y, Ouyang Y, Yang L, Beal MF, McQuibban A, Vogel H, Lu B. 2008.

Pink1 regulates mitochondrial dynamics through interaction with the fission/fusion machinery. Proc Natl Acad Sci U S A. 105(19):7070-7075.

Yao Z, Gandhi S, Burchell VS, Plun-Favreau H, Wood NW, Abramov AY. 2011. Cell metabolism affects selective vulnerability in pink1-associated parkinson's disease. J Cell Sci. 124(Pt 24):4194-4202.

Yu T, Zhao L, Huang X, Ma C, Wang Y, Zhang J, Xuan D. 2016. Enhanced activity of the macrophage m1/m2 phenotypes and phenotypic switch to m1 in periodontal infection. J Periodontol. 87(9):1092-1102.

Zhang J, Wang X, Vikash V, Ye Q, Wu D, Liu Y, Dong W. 2016. Ros and ros-mediated cellular signaling. Oxid Med Cell Longev. 2016:4350965.

Zhang Y, Rohatgi N, Veis DJ, Schilling J, Teitelbaum SL, Zou W. 2018. Pgc1beta organizes the osteoclast cytoskeleton by mitochondrial biogenesis and activation. J Bone Miner Res. 33(6):1114-1125.

Zhao RZ, Jiang S, Zhang L, Yu ZB. 2019. Mitochondrial electron transport chain, ros generation and uncoupling (review). Int J Mol Med. 44(1):3-15.

Zhou L, Zhang YF, Yang FH, Mao HQ, Chen Z, Zhang L. 2021. Mitochondrial DNA leakage induces odontoblast inflammation via the cgas-sting pathway. Cell Commun Signal. 19(1):58.

Zorov DB, Juhaszova M, Sollott SJ. 2014. Mitochondrial reactive oxygen

species (ros) and ros-induced ros release. Physiol Rev. 94(3):909-950.

국문초록

PINK1에 의한 파골세포 분화 조절에 대한 연구

홍 서 진

서울대학교 대학원

치의과학과 분자유전학 전공

(지도교수: 백 정 화, 김 홍 희, 이 장 희)

치주염은 구강 내 박테리아에 의해 발생하는 흔한 만성 질환으로 미토콘드리아 기능 장애와 파골세포 매개의 점진적인 치조골 손실을 동반한다. 최근 연구에 따르면, 적절한 파골세포 분화에는 미토콘드리아 항상성이 필요하다고 한다. 미토콘드리아 전자 수송 사슬 활동의 결함은 미토콘드리아 스트레스를 유발하고 Ca^{2+}-칼시뉴린 매개 미토콘드리아-핵 역행 신호를 활성화하여 결국 파골세포 분화를 증가시킨다.

Mitophagy는 손상된 미토콘드리아를 표적으로 하고 분해하여 산

화 스트레스로부터 세포를 보호하는 필수적인 세포 자가포식 과정이다. 세린/트레오닌 키나아제인 PINK1은 mitophagy를 통한 미토콘드리아 품질 조절에 관여한다. 최근 PINK1이 미토콘드리아 손상으로 인한 과도한 미토콘드리아 Ca^{2+} 유출 및 활성산소종 생성을 방지하는 것과 관련이 있다고 밝혀졌다. 하지만, 파골세포 분화에서 PINK1의 정확한 역할은 아직 밝혀지지 않았다.

본 연구에서 PINK1이 결여된 마우스는 치주염 유도 시, 야생형 마우스에 비해 증가된 치조골 손실을 보였다. 이러한 원인은 분화 및 기능이 증가된 파골세포에 의한 것이라고 가정하였고, 파골세포의 분화 및 파골 능력을 확인한 결과, 야생형 마우스의 파골세포에 비해 분화 및 파골능력이 현저히 증가됨을 확인하였다. 추가적으로, PINK1이 결여된 파골세포에서 미토콘드리아의 손상이 축적되어 있음을 TEM 이미지로 확인하였다. 뿐만 아니라, mitophagy 유도제인 spermidine을 처리 시, PINK1이 결핍된 상황에서 증가되었던 미토콘드리아 손상 및 파골세포 분화 증가의 현상을 억제함을 확인하였다.

종합적으로 본 연구에서는, PINK1의 억제가 미토콘드리아 및 mitophagy의 기능 이상에 관여하여 활성산소의 증가 Ca^{2+}–NFATc1 축을 통해 파골세포의 분화를 촉진하는 역할을 한다는 점을 증명하였다. 따라서, 염증성 및 골 질환 특히, 파골세포 골 손실이 높은 치주 질환에 대한 치료법 개발에 PINK1을 분자 타겟으로 활용하는데 본 연구가 기

여할 수 있을 것으로 사료된다.

주요어: NFATc1, PINK1, 마이토파지, 미토콘드리아, 치주염, 파골세포

학 번: 2016-22040